Medium Modifications of Vector Mesons in the Subthreshold Region

Participants:

G.J. Lolos, Z. Papandreou, E.J. Brash, G.M. Huber,
K. Benslama, S. Dumalski, A. Fleck, N. Knecht, A. Shinozaki, X. Chen
Department of Physics, University of Regina, Regina SK S4S 0A2, Canada

P.L. Cole and A. Larabee
Department of Physics, University of Texas El Paso, El Paso TX 79968

F.J. Klein and S.G. Stepanyan
Thomas Jefferson National Accelerator Facility, Newport News, VA

N. Bianchi, E. De Sanctis, M. Mirazita, V. Muccifora, F. Ronchetti, P. Rossi
INFN-LNS, via E. Fermi 40, I-00044 Frascati, Italy

M. Anghinolfi, M. Battaglieri, P. Corvisiero, M. Ripani, M. Taiuti
INFN-Sezione di Genova e Dipartimento di Fisica dell' Università, I-16146 Genova, Italy

K.Sh. Egiyan, G. Gavalian and Y.G. Sharabian
Yerevan Physics Institute, Yerevan 375036, Armenia

B. Raue
Florida International University, Miami FL 33199

R. Lewis and R.J. van der Meer
Department of Physics, University of Regina, Regina SK S4S 0A2, Canada
and *Thomas Jefferson National Accelerator Facility, Newport News, VA*

A. Afanasev
Dept. of Physics, North Carolina Central University, Durham, NC

B.K. Jennings
TRIUMF, 4004 Wesbrook Mall, Vancouver, British Columbia, Canada V6T 2A3

April 17, 2000

Abstract

We propose to investigate the subthreshold photoproduction of the three lowest mass vector mesons, $V = \rho^0$, ω, and ϕ mesons. In the subthreshold energy region, defined here as the energy region below the $\gamma + N \to V + N$ reaction threshold on the free nucleon, VMD-driven vector meson production is suppressed and the influence of hadronic matter on the masses of the vector mesons is emphasized. This method is the optimum vehicle for the study of in-medium modifications and, specifically for the ρ^0 meson, experimental evidence already exists for a dramatic reduction in m_{ρ^o}, which is dependent on the incident photon energy or the $\rho^0 - N$ relative momentum. This points to a potentially new and unexpected aspect: different regions of phase space enhance, alternatively, the $\rho^0 - N$ and $\rho^0 - A$ interactions and this approach is particularly attractive as a means to separate nucleonic from nuclear (mean field) effects. This assertion will be tested for the $\rho^0 \to \pi^+\pi^-$ channel and the study will be extended also to the unexplored domains of the $\omega \to \pi^+\pi^-\pi^0$ and $\phi \to \pi^+\pi^-\pi^0$ vector mesons. In addition, the hypothesis of vector mesons forming bound states in nuclei will be explored.

An attractive nuclear target for this investigation is ^3He. The minimum trigger requirement is the detection of two charged particles (with an open neutral trigger). We request 420 hours of nominal tagger photon beam ($10^7\gamma/s$) in Hall B, in the tagged photon region between 320 MeV and 1520 MeV, of which 150 hours can be collected in the already approved *g3* period.

This is a Hall B Collaboration experiment.

The Proposal at a Glance

The scientific goals of this proposal are, in order of priority:

1. To carry out definitive measurements on the medium modifications of the ρ^0 meson's mass and width in ^3He and to constrain the numerous theoretical predictions on this subject. In addition, to pursue the separation between nucleonic and nuclear field effects, which is a new finding of the TAGX experiments that is completely unaddressed in the theoretical literature.

2. To measure, for the first time, the medium modification of the mass and width of the ω meson in ^3He and compare it to that of the ρ^0 and to theoretical expectations. In particular, the ω is considered as the ideal vector meson to investigate bound states in nuclei, which also result in mass modifications.

3. To establish the feasibility of extracting the medium modifications of the ϕ, via its pionic decay mode, from remote regions of phase space where the probability of it decaying inside the nuclear medium is maximized.

The main features of the proposed experiment are:

- The above reactions will be pursued in the subthreshold energy regime. This is the most unambiguous and direct manner in which vector meson medium modifications may be probed and the different possible contributing mechanisms identified and separated.

- The ρ^0 production reactions will be $^3He(\gamma_t, V)^3He$, $^3He(\gamma_t, V)p(pn)_{sp}$, and $^3He(\gamma_t, Vp)(pn)_{sp}$ via the $\rho^0 \rightarrow \pi^+\pi^-$ channel, which will be collected with a minimum requirement of two charged pions in the trigger.

- The ω and ϕ reactions will be the same as those for the ρ^0 but via the $\omega \rightarrow \pi^+\pi^-\pi^0$ and $\phi \rightarrow \pi^+\pi^-\pi^0$ channels, with two charged pions in the trigger and the neutral pion as part of an open neutral trigger.

- The tagged photon energy range is: $320 \leq \mathrm{E}_{\gamma_t} \leq 1520$ MeV. The required tagged photon flux is $\geq 10^7\gamma/s$.

- The detector is CLAS in Hall B, which will be optimally operated with the main torus at one quarter strength, B=0.25$B_\circ$.

- We have determined that 420 hours of tagged photon beam on a ^3He target is required for the desired statistical and systematic precision. This beam time does not include DAQ deadtime and any other sources of beam time losses. Our trigger and torus field requirements are partially compatible with those of the *g3* period: 150 hours of beamtime can be common with *g3*, and 270 hours will require dedicated beamtime.

1 Introduction

Recently, much attention has been directed to the coupling of vector mesons to nucleons, especially under conditions of high nuclear matter density where it is expected that this coupling will be modified in comparison to the situation on an unbound nucleon. Clearly, the $\rho^0 - N$ coupling in nuclei, for example, must be known accurately as it is an important ingredient in the calculation of the $N - N$ interaction.

Examples of this interest in vector mesons range from $e - A$ and $\gamma - A$ physics at Jefferson Lab, to relativistic heavy ion collision experiments at CERN, GSI and in the future at RHIC (with an implication on the transition from normal hadronic matter to the conjectured but elusive quark-gluon plasma [1]). The latter has cosmological significance, since the universe was in this deconfined phase a few microseconds after the Big Bang. Other fields of interest include the determination of the equation of state for nuclear matter in connection to the underlying mechanism of supernovae explosions [2] and the properties of remnant neutron stars [3]. All the experiments above involve effects in systems which transit from nucleonic to quark degrees of freedom.

A transition of this nature occurs already in normal nuclear matter. Our aim is to photoproduce the light vector mesons *in the interior* of the nucleus, below the free production threshold, by exploiting the Fermi momentum of nucleons. We will demonstrate that this is the most direct method in the study of in-medium vector meson coupling.

2 Scientific Motivation

2.1 Theoretical Overview

The interior of a nucleus belongs to the long-range and non-perturbative transition region of QCD, which is largely unexplored. Here, QCD-driven interactions among nuclei and mesons affect fundamental particle properties such as masses, lifetimes, and coupling constants. At high hadronic matter temperatures, $T \sim 150$ MeV, lattice QCD calculations [4] support the expectation that the scalar quark (chiral) condensate $< \bar{q}q >$ vanishes, an effect which signifies the transition of nuclear matter from a spontaneously broken symmetry phase to a chirally restored one. However, the condensate itself is not an experimental observable, and therefore other physical quantities associated with it need to be measured to test hadronic medium effects. The masses of the light vector mesons are excellent candidates for this task.

The theoretical basis for mass modification of hadrons in the nuclear medium is overwhelming. Various theoretical methods have been employed in this effort: QCD sum rules (QSR), chiral pertubation theory (χPT), quark-meson coupling (QMC) model, effective Lagrangian theories, Nambu-Jona-Lasinio models, etc. Several review articles have appeared in print on this topic recently [5, 6, 7], and the reader

is referred to the significant number of publications in these review articles. Even though either high temperature T or high nuclear matter density ρ_{nuc} will result in vector meson mass modification, there are significant differences between these two conditions. For the mass modification to take place, the hadronic medium temperature must approach a critical temperature $T_c \sim 150$ MeV [8, 9]. On the other hand, while chiral restoration is expected to take place at nuclear matter densities $\rho \geq 5\ \rho_{nuc}$ [7], substantial changes in the $< \bar{q}q >$ condensate (of $\sim 30\%$) can take place even at normal nuclear matter densities ρ_{nuc}=0.16 fm^{-3}.

In other words, the vacuum energy in the hadron sector must be raised enough to make the quarks massless before the transition can take place. This transition occurs when the scalar field energy reaches a value of 250 MeV/fm^3, which corresponds to an energy density of $\epsilon = 1$ GeV/fm^3 [8]. Such a density can be reached in heavy ion collisions or *inside a nucleon*. Clearly, experiments probing such density effects stand to yield valuable information.

The effect of mass modifications on hadrons has been postulated [10]. This is the original scaling argument by Brown and Rho, who predict that the masses of other light vector mesons scale approximately like those of hadrons:

$$m_N^*/m_N \sim m_\sigma^*/m_\sigma \sim m_V^*/m_V \sim f_\pi^*/f_\pi \tag{1}$$

where the $*$ denotes the medium-modified quantities.

Numerical predictions for the m_V^*/m_V ratio have been produced by a large spectrum of other models. It should be noted that most authors treat the ρ^0 and the ω in the same manner, whereas they quote a different modification of the ϕ meson. The latter is of particular interest since it is modulated by the strangeness content of the nucleon (OZI-breaking parameter), $y = 0.1 - 0.2$, in QCD [11, 12]. The modified masses obey the following relations:

$$m_{\rho,\omega}^*/m_{\rho,\omega} = 1 - (A \pm \delta A)(\rho/\rho_{nuc}) \tag{2}$$

$$m_\phi^*/m_\phi = 1 - (B \pm \delta B)y(\rho/\rho_{nuc}) \tag{3}$$

where

$$y = 2 < \bar{s}s >_N \ / < \bar{u}u + \bar{d}d >_N \tag{4}$$

and the quantities A, δA, B and δB are shown in Table 1. It should be noted that since most models treat the modification ratios A and B in a similar manner, an estimate for y can be obtained by determining A in an experiment and measuring m_ϕ^*/m_ϕ.

The different calculations are in relatively good agreement as far as the ρ^0 and the ω are concerned, with an average decrease of $\sim 20\%$ predicted, at ρ=ρ_{nuc}. A smaller result is predicted for the ϕ [13, 14], although not all authors agree [16]. Nevertheless, a consensus appears to be emerging from the theoretical community

Table 1: Vector Meson Mass Decrement. The uncertainties in the calculations arise from the density dependence of the condensates.

Theoretical Prediction		$m^*_{\rho,\omega}/m_{\rho,\omega}$		m^*_ϕ/m_ϕ	
Model	Reference	A	δA	B	δB
QSR+Walecka	[13]	0.16	0.06	0.15	0.07
QSR+MC	[14]	0.22	0.08	0.06	0.07
QMC	[15]	0.17			
Average		0.18		0.11	

that the masses of the light vector mesons will decrease in nuclear matter, but the extent of the mass modification is still an open question. This is best shown in Figure 1, where the range of the m^*_V/m_V ratio is plotted as a function of the hadronic matter density ratio ρ/ρ_{nuc} as calculated by various QSR based models. Finally, the width of the vector mesons was also found to decrease in QSR [14, 17], as the density increases: for the ρ^0 this implies that the phase space suppression from the $\rho^0 \to \pi^+\pi^-$ process overcomes the collisional broadening at finite density, while an opposite result has been concluded by the work of Klingl et al. [18] who find a large width increase and a small mass change.

The medium modifications described above assume that the vector mesons are on-shell and free (in flight) within the nuclear medium. Very recently, however, another source of mass modification has been postulated, namely that of bound states of the vector mesons in nuclei, in the context of quantum hadrodynamics (QHD) [19]. This theory has met with considerable successes in describing nuclear charge distributions and spin observables in proton-nucleus scattering [20, 21, 22], and involves large scalar (S) and vector (V) fields in the nucleus. These deeply attractive and repulsive fields, respectively, largely cancel out, and their superposition gives rise to the typical nuclear attractive potentials. Nucleons are sensitive to both S and V fields, thus they cannot realize the individual deep field components.

Vector mesons, on the other hand, couple only to S fields and if the vector meson kinetic energy is below that of the binding energy between it and the scalar field, a bound state is formed, and its mass is reduced by the same amount as the binding energy. A recent calculation in reference [23], which is based on the QMC model [15], predicts a large mass modification of the ω, even for as light a nucleus as ^6He, by the formation of a ω-^6He bound state. Furthermore, a different calculation based on QHD and assuming Brown-Rho scaling, as in equation (1), resulted in a large binding energy of the ρ^0 in ^3He. The resultant mass reduction agrees well with experimental results, thus providing evidence that the first such vector meson bound states may have been observed [24].

The physics origins of *bound* vector meson states in nuclei are different than the corresponding ones for mass and/or width modifications expected by the interaction

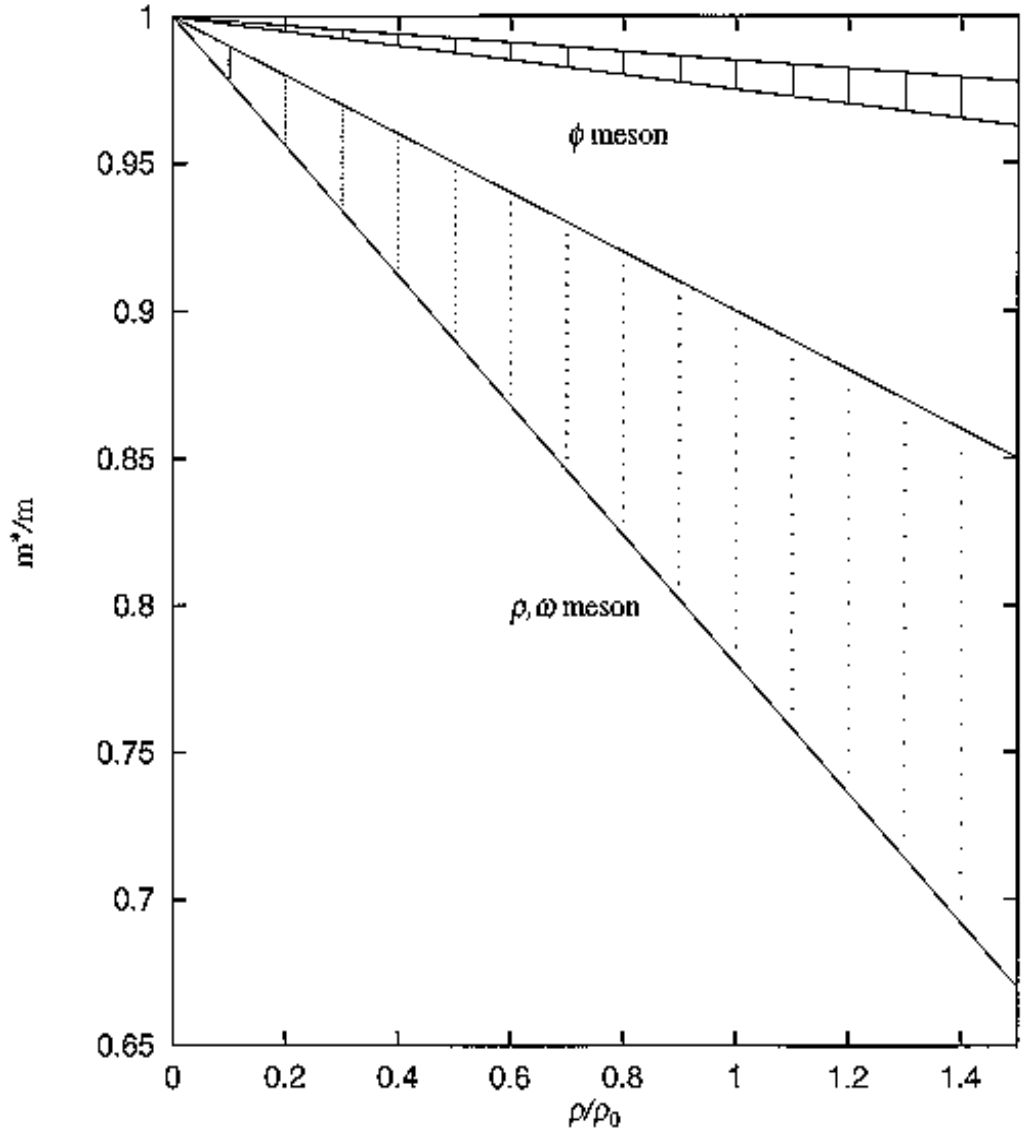

Figure 1: Masses of the ρ^0, ω and ϕ mesons predicted in QSR models [6]. The hatched region expresses the theoretical uncertainties.

of *free* ρ^0 and ω mesons in the interior of nuclear matter. In general, the expected mass modification for bound states is larger than those predicted for the free interaction, at least for normal nuclear matter densities. It is possible, of course, that both phenomena occur in nuclei and this may complicate the interpretation of experimental results.

It is clear that vector meson modifications are expected in some form or another, and while theoretical calculations do cover the whole spectrum of possible mass and width modifications, experimental input is urgently needed.

2.2 Experimental Overview

In Appendix A, we provide the reader with a description of vector meson medium modification results from the last ten years, using hadronic probes. In this subsection, we only highlight these results, and present in more detail what we consider to be the most definitive measurements, carried out with photons. This overview is meant to set the stage for the scientific justification of our proposal.

In Appendix B we compare and contrast the proposed experiment to that of E94-002, approved to run in Hall B, which is similar in its objectives. Finally, in Appendix C we discuss proposed experiments on vector meson medium modifications at various facilities, utilizing different probes and methodology, to impress upon the reader the interest on this topic in diverse subfields of subatomic physics.

2.2.1 Hadronic Probes

There has been a flurry of recent experimental results from a number of accelerator facilities, employing hadronic probes, which have found evidence of a modified ρ^0 meson mass in the nuclear medium. The most notable are: heavy ion collision experiments at CERN, which have seen an unexpected enhancement in dilepton invariant mass spectra at low invariant masses [25, 26, 27]; $K^+ -^{12} C$ elastic cross section measurements at 800 MeV/c that have also revealed an enhancement which may be attributed to a shifted ρ^0 mass [28]; and a $\vec{p} - A$ scattering experiment at IUCF that has evoked shifted meson masses in an attempt to explain spin-transfer observables [29]. Although these types of experiments have inferred the presence of medium modifications, they were not entirely conclusive, as other conventional mechanisms could also explain the data, at least in part.

2.2.2 Photon Probes

The first "direct" measurement of the ρ^0 mass modification was performed at INS-ES, via the photoproduction reaction $^3He(\gamma_t, \rho^0 \rightarrow \pi^+\pi^-)$, with tagged photons in the energy range 800-1120 MeV and with the two pions detected in the TAGX[1]

[1]For the interested reader, a detailed description of the TAGX System is presented in reference [30].

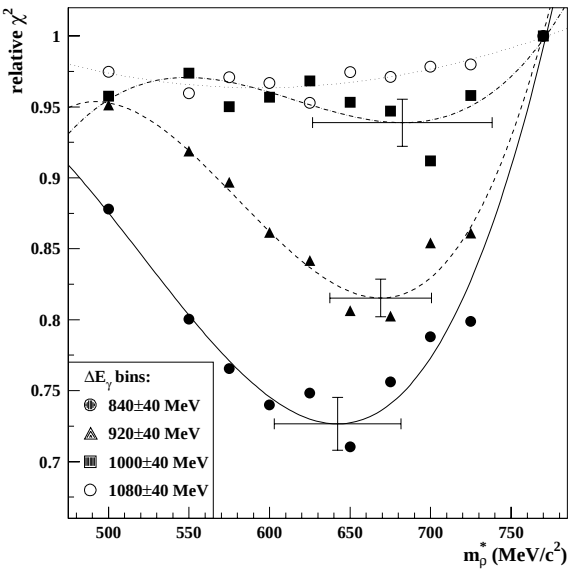

Figure 2: The dependence of the χ^2 as a function of $m^*_{\rho^o}$, resulting from the MC fitting to the data [33], for four different tagged photon energy bins. The MC calculations are indicated as points, and the curves display third-order polynomial fits to these points. The extracted masses from the two lowest curves are 642±40 MeV/c^2 and 669±32 MeV/c^2 for the 800-880 MeV and 880-960 MeV tagged photon energy bins, respectively.

magnetic spectrometer. The analysis was consistent with a 17% reduction in the ρ^0 mass [31], which is illustrated in Figure 2. A subsequent reanalysis of older TAGX double-pion production results, at lower tagged photon energies (380-700 MeV), confirmed the large mass shift [32]. Moreover, the characteristic p-wave distribution of the $\rho^0 \rightarrow \pi^+\pi^-$ decay has been observed and is shown in Figure 3, further assuring the validity of the ρ^0 signature among all the competing channels [33]. This p-wave signature only manifests itself in the 500-600 and 600-700 MeV/c^2 invariant mass regions, as seen in panels (b) and (c) of this figure, clearly indicating that the mass of the ρ^0 is shifted from its free value of 770 MeV/c^2. The conclusions from reference [31] were that the reduction, δm_{ρ^0}, of the ρ^0 mass was much larger than any theoretical prediction, and that the mass shift increased as the experiment probed deeper below threshold. This analysis will be discussed in further detail in Section 4.2, as it will form the basis for the analysis of the experiment proposed here.

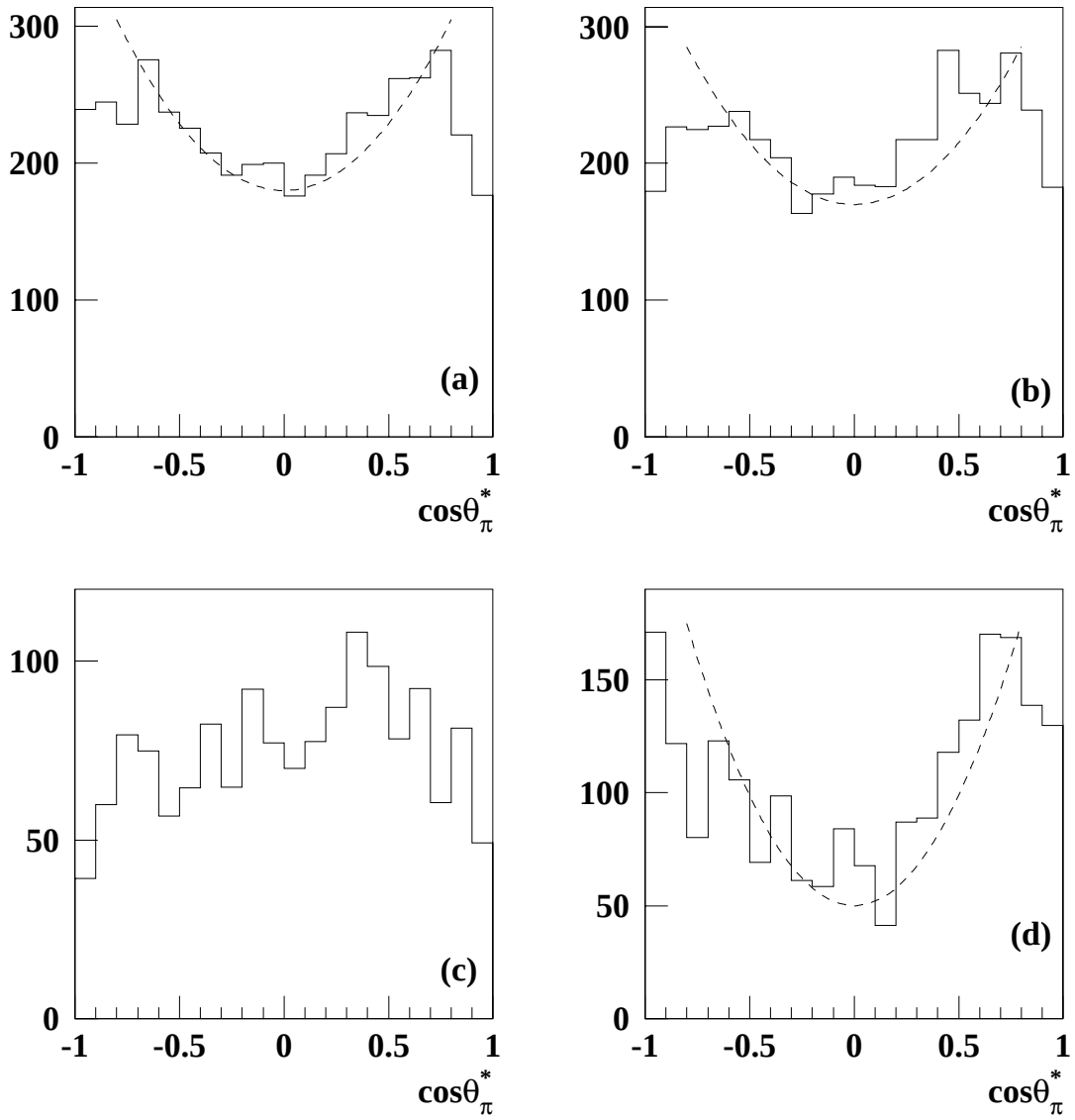

Figure 3: The $\cos\theta^*_{\pi^+}$ distribution is shown in the invariant mass regions of a) 500-600 MeV/c^2, b) 600-700 MeV/c^2, c) 700-800 MeV/c^2 and d) 500-600 MeV/c^2 after a subtraction of the 'flat' 400-500 MeV/c^2 distribution. Panels a), b) and d) capture the $l = 1$ signature of the $\rho^0 \to \pi^+\pi^-$ decay.

3 Physics Objectives of this Proposal

The principal properties of the three lowest mass vector mesons are displayed in Table 2, with the boxed numbers indicating the decay modes that will be measured in this experiment.

Table 2: Vector Meson Properties

Particle (MeV/c^2)	Width (MeV/c^2)	$c\tau$ fm	BR($\pi^+\pi^-$) %	BR(3π) %	BR($\rho\pi$) %	BR(e^+e^-) %
ρ^0 (770)	~ 151	1.3	$\boxed{\sim 100}$	$< 1.2 \times 10^{-2}$	-	4.5×10^{-3}
ω (782)	~ 8.5	24	2.2	$\boxed{\sim 89}$	-	7.1×10^{-3}
ϕ (1020)	~ 4.5	45	8×10^{-3}	$\boxed{2.5}$	$\boxed{\sim 13}$	3×10^{-2}

We begin by reiterating the aims behind the study of each of the three vector mesons. We stress that different emphasis and priority is placed on each meson, with the ρ^0 and ω comprising the main objectives of our study, as will be explained in detail below.

- *The ρ^0 meson:* We seek to provide quantitative and definitive information on the physics origin (nuclear or nucleonic) of the downward shift of the mass of this meson - as compared to its vacuum value. From our TAGX experience, we are confident that the extraction of this information will be accomplished with a high certainty and will be much more constraining to theory than the TAGX results, which had certain limitations, as explained further in Section 4. Clearly, since the ρ^0 has a short decay length, its populated phase space related to medium modifications will be large, which implies that any modifications measured will carry a high confidence. However, due to the large width of this resonance and the broad shapes of competing mechanisms, a small modification of its width may not become readily apparent. In the process, this will exclude theoretical claims of minimal mass but large width effects. Depending on the invariant mass binning that can be achieved, the experiment will be sensitive to a change in $\delta\Gamma_{\rho^0}$ as low as 20 MeV/c^2.

- *The ω meson:* This particle has not been investigated as far as medium modifications are concerned. Whereas some models expect the ρ^0 and ω masses to be similarly modified [11, 14], others predict a smaller mass decrease for the ω [34]. Furthermore, the small width of the ω and its three-pion decay mode is a unique signature among mechanisms in its mass range and establishes it as a sensitive probe of even small mass and/or width modifications. This comes at the expense of reduced in medium decay probabilities, which, with some care, can be enhanced in selected regions of phase space.

It is, however, the investigation of the bound state of vector mesons in nuclei which places additional emphasis on the photoproduction of the ω meson. A bound ω will result in nearly 100% in medium decay probability *if produced essentially at rest or with very low momentum with respect to the nucleus.* The long in-flight decay length of the free ω in the nucleus, even at very low kinetic energies, will result in a small number of modified ω mesons, while a bound state will result in a large fraction with respect to natural mass ω decaying outside of the nuclear medium. Thus, the observed fraction of modified to unmodified detected ω mesons will separate these two different effects. Furthermore, unlike the in-flight modifications which have an energy dependence as a function of effective $\gamma\beta c\tau$, bound states exhibit more or less a *threshold* type of energy dependence as either bound or free ω mesons within the nuclear S field. Clearly, under these conditions, the ω is the ideal vehicle to probe such bound states in nuclei.

- *The ϕ meson: QSR* predict a decrease in the ϕ mass, which is further modulated by the strangeness content of the nucleon (see equations (3) and (4)). In addition, as a pure $\bar{s}s$ state, the ϕ is sensitive to the $<\bar{g}g>$ gluon condensate, and thus the scope of medium modifications is expanded by including gluonic contributions to the interaction matrix elements [35]. Specifically, it has been shown that if a first order QCD phase transition occurs in ultrarelativistic heavy ion colisions, a double ϕ peak will appear in the dilepton invariant mass spectrum. This peak persists even when the transition from quark to hadronic degrees of freedom is a smooth crossover, and as such the double peak is a viable signal for the formation of quark-gluon plasma [36]. Having stated this, however, it should be emphasized that it is unknown whether such a peak will manifest itself in the chiral transition accessible in the subthreshold region of this experiment. Furthermore, the populated phase space production of the ϕ is very small, and whether it is realistically measurable depends on the statistics we will be able to accumulate in remote regions of phase space. The drawbacks notwithstanding, the physics motivation of ϕ mass modifications is compelling enough to warrant a serious look, in the very least, at the possibilities and limitations. Our aim in this regard is to perform a feasibility study which will serve as input to future experiments.

We propose to use CLAS to investigate the ${}^3He(\gamma_t, V){}^3He$, ${}^3He(\gamma_t, V)p(pn)_{sp}$, and ${}^3He(\gamma_t, Vp)(pn)_{sp}$ reactions, where $V = \rho^0$, ω, or ϕ mesons, by detecting the hadronic decay modes indicated in Table 2. These modes were selected over the leptonic ones mainly because of their favorable branching ratios. Clearly, each reaction channel and each vector meson probe different aspects of medium modifications. Fortunately, the data for all these will be accumulated simultaneously in CLAS. The choices of ${}^3He$ as the nuclear target and 320-1520 MeV tagged photon energy contribute to the suppression of competing channels, including those which involve final state interactions of the decay hadrons.

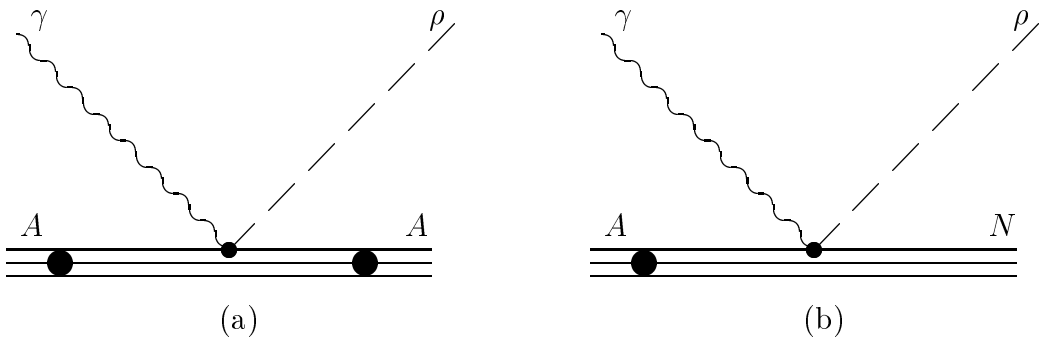

Figure 4: Diagrams contributing to the ρ^o meson channel: (a) and (b) refer to the exclusive and breakup channels in the text, respectively, and contribute in the subthreshold region.

3.1 Vector Meson Production in the Subthreshold Region

The general physics topic of our proposal is similar to that of proposal E94-002 [37], however, *the subthreshold emphasis in this proposal is unique.* A detailed comparison of the two methods is outlined in Appendix B.

The diagrams that contribute to the vector meson production processes of interest to this proposal are shown in Figure 4. The interaction vertex can be driven by the exchange of a pomeron, pion or vector meson. The exact mechanism, which depends on the four-momentum transfer, is not relevant to the investigation of this proposal; rather, only the kinematics of the reaction and the final state are of interest here, since the physics of vector meson medium modifications alone already define the scientific motivation of this proposal.

Above the threshold of vector meson photoproduction off a proton, the single nucleon amplitudes contribute coherently to the total vector meson production cross sections on nuclei, and as a result yield large cross sections. This was verified by ρ^0 production on nuclei at photon energies in the 2.6-6.8 GeV region [38]. However, in that energy region, where the momentum transfer to the struck nucleon is very small, ρ^0 mass modifications could not have been observed for two reasons: *first*, as $t \to 0$ in coherent (diffractive) ρ^0 production, the ρ^0-mesons are produced essentially outside the nucleus and only a fraction of them is expected to penetrate its interior region; *second*, among the ones that do penetrate, only a very small fraction will decay within the nuclear volume due to the $\gamma\beta c\tau$ factor. The latter argument is even more compelling for the ω and ϕ mesons, which have $c\tau$ factors of 24 fm and 45 fm, respectively.

This effect is clearly illustrated in Table 3, for 5 GeV photons impinging on a ^3He nucleus as compared to the 1 GeV case. Clearly, any attempt to produce vector mesons off nuclei significantly above threshold greatly decreases the sensitivity to

medium modification effects.

Table 3: Fraction of ρ^0 , ω and ϕ decays inside each nucleus, $f = (1 - e^{-\frac{R_A}{\gamma c\tau}})$.

E_γ	Target	R_A $[fm]$	$\gamma_{\rho,\omega}$	$\gamma_\rho c\tau[fm]$	f_ρ (%)	f_ω (%)	$f_\phi^\dagger$ (%)
5 GeV	^3He	1.7	6.51	8.46	18	1.1	0.8
1 GeV	^3He	1.7	1.23	1.60	66	5.6	3.5
1 GeV	^4He	1.9	1.24	1.61	70	6.2	3.7
1 GeV	^{12}C	2.74	1.29	1.68	80	8.5	5.1
1 GeV	^{208}Pb	7.11	1.29	1.68	99	21	12.5
† E_γ is 1.2 GeV for the ϕ meson.							

On the other hand, below the photoproduction threshold on a free nucleon, termed the **subthreshold region**, we essentially "force" the interaction vertex to occur within the nuclear volume, thus enhancing the probability of medium modifications. In this situation, the vector meson can be brought on-shell mainly in one of two ways:

1. By employing a small momentum transfer in the reaction, one probes primarily the low region of the Fermi-momentum distribution of the participating nucleon. This process is mainly associated with a bound ^3He nucleus in the final state, as shown in Figure 4(a). We term this as the **exclusive** channel and a mass modification is essentially a nuclear mean field effect. This is done in order to avoid confusion with the same reaction above threshold, which is termed the coherent production. As the momentum transfer increases in the subthreshold region, the exclusive cross section decreases rapidly, falling with the ^3He elastic form factor. The ρ^0, of course, can also be produced coherently, but at $E_\gamma = 840$ MeV, for example, only half of the ρ^0 resonance mass can be populated, which means that this process is suppressed.

2. By requiring a large four-momentum transfer in the reaction, compared to the average single (bound) nucleon's Fermi four-momentum, the region of large momentum components in the single nucleon wavefunction is probed. This process is represented diagramatically in Figure 4(b). This, of course, results in small cross sections, compared to the total ρ^0 cross section *above threshold*, but nevertheless it dominates the cross section in the subthreshold regime, and corresponds to a short-distance $\gamma - N$ interaction. We refer to this reaction as the **breakup** channel and medium modifications are dependant on the field of the interacting nucleon, due to the short-range nature of the interaction.

An additional and important benefit of subthreshold production is connected to the low photon energy employed. This involves a small Lorentz boost from the

center-of-mass to the lab frame and thus vector mesons emerge with small velocities relative to the participating nucleon (nucleus), which results in an increased probability of the vector meson decaying *within* the nucleonic (or nuclear) field. This is dramatically illustrated in Figure 5. Furthermore, the small kinetic energies of the produced ρ^0 and ω will also allow the investigation of possible bound states in ^3He. Such investigations can effectively take place only at threshold or subthreshold energy regimes to assure the formation of bound states.

In short, in our proposed experiment we aim to selectively examine regions of phase space where diagrams 4(a) and 4(b) are alternatively enhanced/suppressed, as they probe nuclear versus nucleonic field modifications, respectively. Both channels will be presented in further detail, following the discussion on the target nucleus. It should be emphasized here that the physics nature of the nuclear and nucleonic medium modifications is the same. The only difference is the effect each has on the magnitude of the measured final mass modification.

3.2 The Choice of Nuclear Target

In principle, one desires as massive a target as possible (high ρ_{nuc} and large charge distribution radius) in order to amplify the expected nuclear medium modifications. However, in subthreshold production, where the vector meson is produced essentially at rest, the fraction of in-medium decays is high enough for light nuclei that a heavy nuclear target does not provide much of an advantage, as is evident in Table 3 and Figure 5. This point is also reflected in the expected mass modification of the ρ^0 in a finite nuclear density distribution as calculated in [39]. In this reference, unlike all other calculations which involve infinite nuclear matter, the experimentally parameterized charge density distributions for ^3He, ^4He, and ^{12}C were used. The values of δm_{ρ^0} were calculated to be 40, 80, and 50 MeV/c^2, respectively. In other words, the mass modification difference between ^3He and ^{12}C is not significant, while the larger one for ^4He reflects its higher core density. Additionally, in the context of final state interactions (FSI), a heavy target is disadvantageous for hadronic decays which, for the three vector mesons in this proposal, dominate the branching ratios. Finally, if the large δm_{ρ^0} observed in the TAGX results is indeed nucleonic in origin, nuclear size will not matter.

The chosen target, ^3He, is an attractive choice on physics grounds, and it also allows a direct comparison with the TAGX results. There is an additional, practical reason why ^3He is the ideal *first* nuclear target for the study of the modifications of vector mesons: the scientific motivation of E93-044 [40] is centered on the investigation of all photoreaction channels (except subthreshold vector meson production). In essence, the foreground reactions of E93-044 are our background channels. Such an ideal symbiosis of experiments is only achievable with the CLAS spectrometer in Hall B.

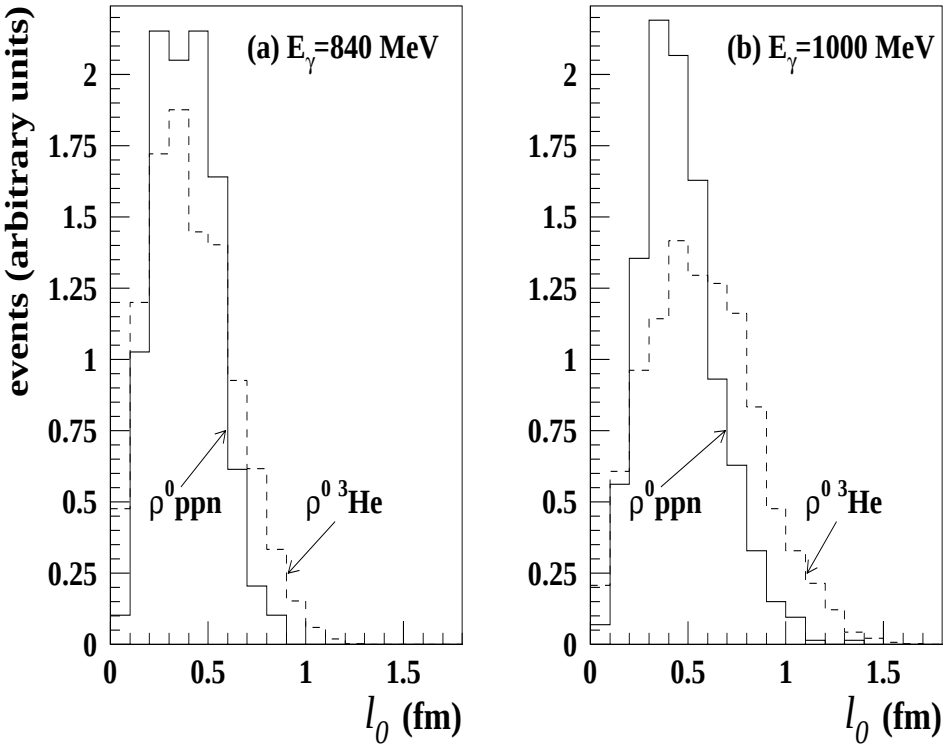

Figure 5: Simulated mean decay length l_0 distribution, of the $\rho^0 \to \pi^+\pi^-$ decay, is indicative of the distances probed for vector meson modifications in the TAGX experiment. The l_0 spectra are illustrated for a) $E_\gamma = 840$ MeV and b) $E_\gamma = 1000$ MeV. The histograms are for MC generated events accepted by the spectrometer in the $^3He(\gamma_t, \rho^0)p(pn)_{sp}$ (solid curves) and $^3He(\gamma_t, \rho^0)^3He$ (dashed curves) reactions, normalized to unity. The mean decay length is for the former reaction in the rest frame of the participating proton (the two remaining nucleons being spectators), and for the latter in the rest frame of the ^3He nucleus.

3.3 The Exclusive $^3He(\gamma_t, V)^3He$ Channel

This reaction, for the ρ^0 and ω, is one of our two primary objectives.

The exclusive reaction is, in principle, the most sensitive way to investigate vector meson medium modifications in the *mean field* of the nucleus. We refer to this as the **nuclear effect**. As a test of the theoretical calculations, this is the reaction to compare with, at least for light nuclei.

Here the aim is to isolate diagram 4(a), which constitutes 15% of the cross section at subthreshold energies. This is accomplished by imposing selection criteria on the missing mass spectra, as will be explained in detail in Section 4.2. This, in effect, allows access to regions of phase space where the relative velocity between the produced vector meson and the intact nucleus maximizes the probability of the meson decaying within the nuclear density distribution, as shown in Figure 5.

The TAGX experiments [31, 32] spurred specific theoretical calculations, based on the QMC model of Saito, Tsushima and Thomas [39, 41]. The results of the calculation for ^3He were consistent with $\delta m_{\rho^0} = 40$ MeV/c^2, which is much smaller than the extracted values from the TAGX experiments of 130 and 250 MeV/c^2, corresponding to 800-1120 MeV and 380-700 MeV tagged photon energies, respectively. Figure 6 shows the calculations for ^3He. Since the ^3He nucleus has a radius of 1.7 fm and a mean density equal to 0.4 ρ_{nuc}, the calculation predicts a mass modification of about 8%, whereas the data supports a number closer to 17%. This discrepancy is significant and must be pursued further with CLAS, since the model of Saito et al. includes an explicit parameterization of finite nuclear properties.

3.4 $^3He(\gamma_t, V)p(pn)_{sp}$ and $^3He(\gamma_t, Vp)(pn)_{sp}$ Breakup Reactions

This reaction, for the ρ^0 and ω, is the second of our two primary objectives.

As reported in references [31, 32, 33], the breakup reaction in diagram 4(b) dominates the total ρ^0 photoproduction cross section in the deep-subthreshold region, and the obtained dramatic ρ^0 mass modification results are consistent with the onset of a new mechanism. Specifically, the relative momentum between the ρ^0 and the struck nucleon is such that the majority of the ρ^0 particles will decay within the hadronic field of the nucleon [42]. As an example, for the lowest TAGX energies, the mean decay length between the produced ρ^0 and the struck nucleon is approximately 0.3 fm. In essence, the ρ^0 decays at its production vertex [32]. Even at $E_\gamma =$ 840 MeV, approximately 70% of the produced ρ^0 mesons decay within 0.5 fm from the production vertex, as shown in Figure 5.

In this situation, nuclear matter density considerations like those reported in reference [39] are not relevant, but the nucleonic density may be at play instead [42]. These conclusions seem to be supported by the findings of reference [8], in which energy densities of 1 GeV/fm^3 result in chiral symmetry restoration. Such densities are manifested within the nucleonic domain. It turns out that, at $V - N$ relative coordinates of 0.5 fm or less, the nucleon's hadron matter density is high enough

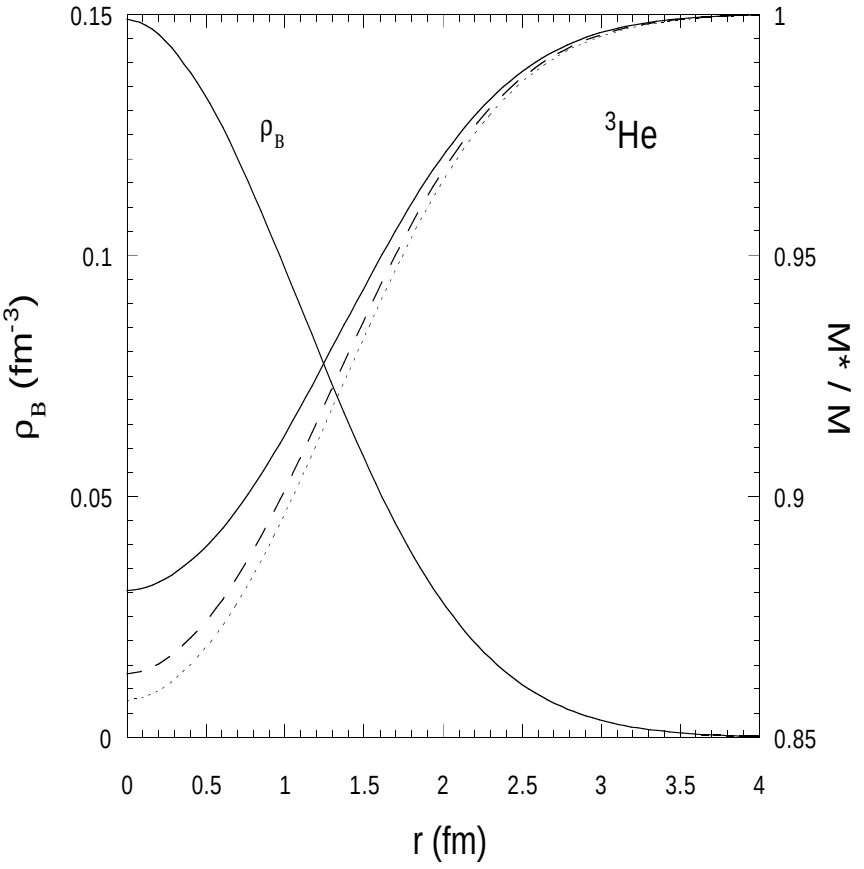

Figure 6: The modified to unmodified mass ratio for the ρ^0 meson, as a function of nuclear radius, from reference [39].

to exceed ρ_{nuc}, and thus induce a mass modification that cannot be realized in the context of the nuclear mean field. If this is indeed the case, in deeply subthreshold vector meson production, the mass modification should be nearly independent of mass number. This **nucleonic effect** has not been considered in any of the theoretical calculations, and has been reported for the first time in reference [31]. The experiment planned with CLAS will greatly increase the confidence in the separation of these two different diagrams.

For the other two mesons, due to their longer $c\tau$, it is even more critical to be selective in terms of phase space, in order to probe low $V - N$ relative velocities. In these regions, we not only expect to maximize the mass modification but to also increase the ratio of modified to unmodified V-mesons, as well. For the bound ω case, the final state will follow a six-body phase-space distribution, unlike the ω reaction in Section 3.3 which follows a four-body distribution.

3.5 Future directions

The results of the proposed experiment will resolve the issue of the nucleonic modification of the ρ^0 and ω and will determine the magnitude of the modifications more reliably than the TAGX results have for the ρ^0 meson. They will also deconvolute the contributions of $\delta\Gamma_{\rho^0}$ and δm_{ρ^0} to the overall (compounded) $m^*_{\rho^o}$ extracted from the TAGX analysis. As an extension of the investigation of the nuclear density effect of ρ^0 and ω modification (via the exclusive reaction), a next logical target would be ^4He, for its simplicitly and high nuclear density. The separation of exclusive and breakup channels, in particular, is much simplified by the 22 MeV separation between the ^4He ground state and the onset of excitations and break up. While an experiment on ^2H and ^{12}C has been completed at INS-ES using the TAGX detector, the advantages of CLAS dictate that these investigations need to be pursued as a function of mass number for selected light nuclei.

Although the emphasis of this experiment is *the investigation of the* ρ^0 *and* ω *mass modification*, we will also attempt to extract similar information on the ϕ meson. A successful outcome in the latter case will naturally lead to future dedicated experiments.

The next candidate in this search is the J/ψ. It has been predicted that J/ψ suppresion would unambiguously signal quark gluon plasma formation. There is an extensive set of measurements from experiments NA38 and NA50 at CERN [43] that indicates that the J/ψ production rate is suppressed by nearly a factor of two with respect to the Drell-Yan production cross section. It has been suggested that this is evidence of the onset of a new, very dense state of matter. At JLab/Hall B, further down the road, similar investigations with the *subthreshold production* of the J/ψ open up. These will allow us to reach into the $c\bar{c}$-interactions with the nuclear medium [35].

In this context, the present proposal is the first step towards a potentially rich program of investigations of subnucleonic degrees of freedom in the nuclear medium, thus fulfilling the original statement of this physics as one of the last frontiers of QCD. These experiments are not easy and the analysis of the data is very complex. A step by step approach is required, building the case of each experiment on the solid results of the previous one.

4 Experimental Methodology at Hall B

4.1 Comparison of INS-ES and Hall B Systems

Beam: The maximum endpoint energy of INS-ES is 1.22 GeV. This precludes the mapping of the ϕ meson, which can be achieved in Hall B. Furthemore, the quality of the electron beam at JLab far exceeds that of INS-ES (a 100% duty factor as opposed to 10% at INS-ES) which shortens the running period and makes it easier to control the systematics.

Tagged Photons: The Hall B tagger can provide a flux of $10^7\gamma/s$, nearly two orders of magnitude improvement over the INS-ES facility. This will allow the accumulation of statistically significant data in regions of phase space where the physics are particularly interesting and otherwise inaccessible. It will also allow for a finer tagged photon energy binning than used in the TAGX analysis, which will further constrain the MC simulations, reduce uncertainties in the assumed constancy of the matrix elements, and significantly improve the reliability of the MC fits to the data.

Acceptance and Coplanarity: A nearly 4π sr detector like CLAS has both advantages and disadvantages over a 1π sr device such as TAGX. In the latter case, the restricted, in-plane coverage simplified the extraction of the ρ^0 channel from competing data, as this is the only inherently coplanar $\pi^+\pi^-$ process in this energy range. By presenting a small overall acceptance for two-step processes and double-pion production due to multibody phase space processes, TAGX naturally suppressed such background [32].

Once this is accomplished, however, the limited out-of-plane acceptance makes extrapolations over unmeasured regions of phase space somewhat uncertain. In fact, our fitting procedure relied on such extrapolations: agreement with total cross sections from the literature was used as a constraint to the fits, and this translated in a large uncertainty in the determination of δm_{ρ^0}. CLAS may not improve the $\rho^0 \to \pi^+\pi^-$ detection all that much over TAGX, but the experimental confidence associated with the actual detection of Δ and N^* decay products out of plane will be invaluable in the final determination of δm_{ρ^0}, without the uncertainties present in the TAGX results. Moreover, ω detection capability eluded TAGX, while it will be quite satisfactory with CLAS, due to its neutral capability in detecting the two photons from the $\pi^0 \to \gamma\gamma$ decay.

One should also note that, in selected regions of phase space, the participating nucleon can also be detected in CLAS, which will further enhance the reliability in reconstructing the reaction and assuring kinematical completeness, as discussed in Section 4.2 below. This feature is valuable in the definition of coplanarity and missing momentum criteria, which are powerful signatures for the ρ^0 production process.

Resolution: The resolution of TAGX is approximately 3.5% $\Delta p/p$ for pions of 350 MeV/c momenta. The CLAS momentum resolution (ca. 1%) will allow a more precise determination of the particle tracks, which will result in an even "cleaner" data set, as the PID definition is expected to be sharper than that of TAGX. This will undoubtedly aid in the separation of the ω from the ρ^0 and will also have advantages in the missing energy spectrum. If any conclusions could be drawn from the data on a possible ϕ mass modification, the available resolution with CLAS will play an important role. Finally, it is certain that an investigation of mass modification as a function of $V - N$ relative momenta (or coordinates) requires the high statistical precision and resolution achievable only in Hall B. The large in- and out-of-plane coverage of CLAS will also provide angular distributions which will assist in the

deconvolution of the data.

Conclusions: Clearly, the advantages of the Hall B/CLAS system are numerous. The proposed experiment will address the new effects in ρ^0 mass modifications suggested by the TAGX results, and improve the quality of the results on vector meson medium modifications substantially over the existing TAGX data, while allowing a careful study of both ω and ϕ mesons that was not feasible at INS-ES.

4.2 Extraction of the V mass from the data

At present, we propose to extract the modified vector meson mass from the CLAS data in a manner similar to our already published TAGX analyses [31, 32, 33]. Our analysis method is under constant refinement, and any subsequent improvements will be considered and incorporated in the CLAS analysis. For the sake of brevity, the following discussion will consider V= ρ^0 only.

As will be explained below, we plan to analyze two-, three- and four-track CLAS data, including $\pi^+\pi^-$, $\pi^+\pi^- p$ and $\pi^+\pi^- p(p)$ events, in addition to events containing a detected π^o. This is because the different physics processes which contribute significantly to $\pi^+\pi^-$ photoproduction in this energy region can also result in the emission of one or more energetic nucleons. *The extraction of these multitrack data, from the large CLAS acceptance, together with the greatly improved statistical precision, will provide a striking advance over the previous TAGX experiment.*

The particles will be identified from the TOF versus momentum information, as shown in Figure 7. From this figure we see that protons (upper band) and pions (lower band) are cleanly separated.

In the remainder of this section, we will present the physics background processes, the cuts which reduce their contribution to the data, and the analysis philosophy to isolate the ρ^0 contribution from both the $\pi^+\pi^-$ and $\pi^+\pi^- p$ event samples.

4.2.1 Physics Background Processes

Briefly, the physics background processes that we have to consider here are:

- $^3He(\gamma, \Delta\pi)$ on a nucleon, followed by $\Delta\pi \rightarrow \pi^+\pi^- N$ (the two other nucleons are spectators). This is the dominant $\pi^+\pi^-$ production mechanism in the 1 GeV region [44]. As this process usually results in the emission of an energetic nucleon, it will contribute to both the two- and three-track event samples.

- Quasifree N^* production, $^3He(\gamma, N^*\pi)$ on a nucleon, which decays via either $N^* \rightarrow \pi N$ or $N^* \rightarrow \Delta\pi \rightarrow \pi\pi N$. Here N^* includes the Roper, the N^*_{1520}, and other higher nucleonic resonances, as appropriate. These processes gain importance as the incident photon energy is raised to the 1-1.5 GeV region, otherwise they are similar to the quasifree $\Delta\pi$ channel.

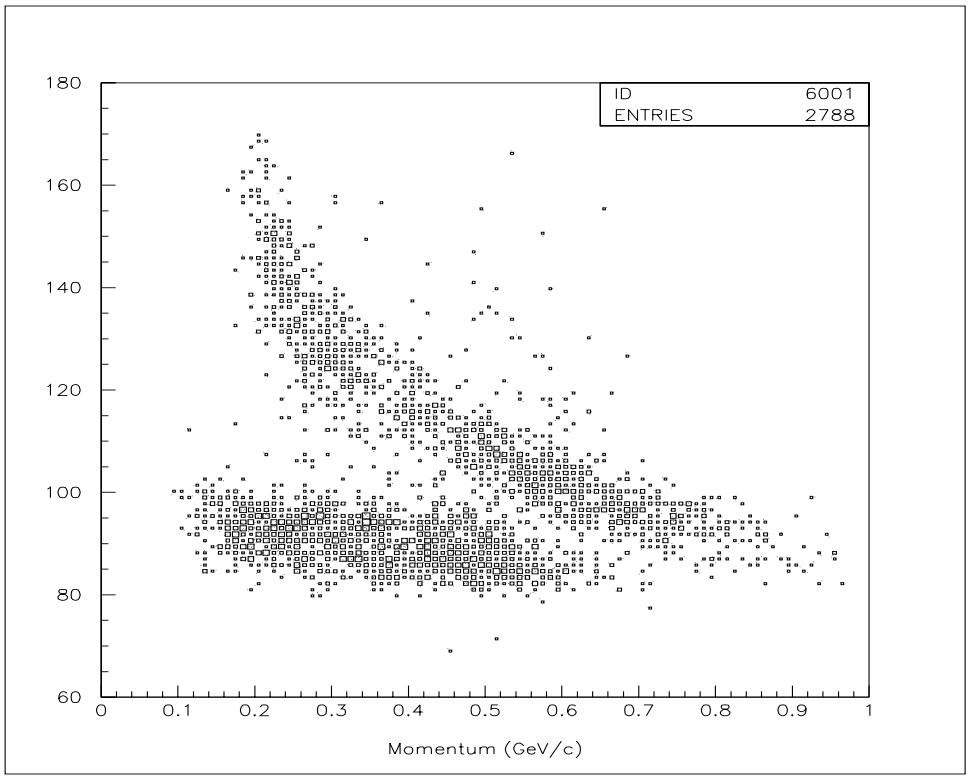

Figure 7: Simulated TOF versus momentum for CLAS. The upper band is protons and the lower band is pions. Some muons (below the pion band) are visible.

- $^3He(\gamma, \Delta\Delta)$ on a nucleon pair, followed by $\Delta\Delta \rightarrow \pi^+\pi^- NN$. This reaction has been measured on both ^2H [45, 46] and ^3He [47] targets, and is the second most important process at 1 GeV.

- Incoherent $\pi^+\pi^-\pi^0$ production. At 1 GeV, this channel is fairly weak, but at TAGX it was found to contribute to the high missing momentum region (the π^0 escaped undetected). The neutrals capability of CLAS should aid in the understanding of this portion of the data set, and will be especially helpful in the ω and ϕ analyses.

- Final state interactions, of the form $\pi N \rightarrow \pi' N'$, can occur between the pion produced from ρ^0 decay and one of the nucleons, possibly mimicking the signature of a medium modified ρ^0 mass, and leading to an erroneous conclusion. Therefore, this process (for an unmodified ρ^0 mass) will be modelled and included in the fitting procedure. However, ^3He was chosen as a target in order to minimize FSI complications, and the TAGX analysis has confirmed that the contribution of the FSI process to the data is minimal. The issue of FSI will be dealth with, in more detail, in Section 4.2.4.

4.2.2 Analysis of the $\pi^+\pi^-$ Events

The analysis of these CLAS events will be very similar in philosophy to the TAGX analysis [31, 32, 33]. Our $^3He(\gamma_t, V)$ foreground processes have significantly smaller cross section than the sum of those listed above. However, there are several factors in our favor which will greatly ease the extraction of the ρ^0 signature from the data:

1. The $\rho^0 \rightarrow \pi^+\pi^-$ process is intrinsically coplanar, whereas the background processes listed above generate noncoplanar as well as coplanar pion pairs. Cuts on the relative azimuthal angles will be placed on the data, to take advantage of this natural feature. In the case of $\omega \rightarrow \pi^+\pi^-\pi^0$ and $\phi \rightarrow \pi^+\pi^-\pi^0$ channels, four-momentum and invariant mass criteria, coupled to the narrow width of these resonances, will suffice to suppress the background processes even without the coplanarity criteria.

2. A cut on the opening angle between the two pions preferentially selects pions from the ρ^0 decay, since the pions emerge back-to-back in the ρ^0 rest frame.

3. A cut on missing mass can be placed to separate the contributions of the $^3He(\gamma_t, V)^3He$ and $^3He(\gamma_t, V)p(pn)_{sp}$ channels.

4. Simulated events from foreground as well as background processes, having taken into account the effects of detection threshold and finite acceptance, will be fit to the data. The vacuum values for the masses and widths of all resonances will be used in the simulations, with the exception of the ρ^0 meson, for which simulations with both free and modified mass and width will be carried out. The MC fitting procedure is expounded below.

MC Fitting Procedure

The MC physics generators are purely phase-space driven, in the sense that the matrix element is constant in each narrow tagged photon energy bin. As with the TAGX analysis, the fitting procedure will be an *iterative and simultaneous fitting of several experimental observables*, with the data from each photon energy bin *treated completely independently of the others.*

These experimental observables are: the dipion invariant mass $m_{\pi\pi}$, the missing mass m_{miss}, the opening angle between the two pions $\theta_{\pi\pi}$, the missing momentum p_{miss}, the emission angle of the $\pi\pi$ system θ_{IM}, and the cosine of the pion angle, θ^*_π, in the dipion rest frame. The fitting will also be carried out simultaneously in three missing mass regions, one focusing on the breakup channel of ^3He, one on the exclusive (^3He) region, and the final one unrestricted. Such a fit is not optimized just on the $\pi^+\pi^-$ invariant mass, as with the CERES analysis, but takes into account the distribution of the data over a wide range of experimental observables. This intends to reduce the chance of a fortuitous fitting to the data, and the extraction

of an erroneous modified ρ^0 invariant mass. Essentially, we plan to take advantage of the full power of the data set obtainable with a large solid angle detector.

For the TAGX analysis, we simulated the $^3He(\gamma_t, V)^3He$ and $^3He(\gamma_t, V)p(pn)_{sp}$ final states with several different shifted ρ^0 masses from 500-725 MeV/c^2. The goodness of fit was calculated for each combination of free and modified ρ^0 masses, and it was found that the best fit was obtained with a reduced ρ^0 mass of approximately 642±40 MeV/c^2 and 669±32 MeV/c^2 for the 800-880 MeV and 880-960 MeV tagged photon energy bins, respectively, (see Figure 2) and a free width. However, a combination of smaller mass modification accompanied by substantial width modification [18] is also consistent with the data [33]. Finally, we observed $\rho^0 \rightarrow \pi^+\pi^-$ contributions from both modified and free mass ρ^0 mesons in the same data set, as expected if the ρ^0 is sometimes produced and decays in the ^3He interior (resulting in an observed mass reduction), and is sometimes produced and decays on the ^3He periphery (resulting in little or no mass shift). The interested reader is referred to [31, 32, 33, 47] for additional details of the INS-ES analysis.

4.2.3 Analysis of the $\pi^+\pi^-p(p)$ Events

In addition to the $\pi^+\pi^-$ method described in the previous section, in the analysis of the CLAS $\pi^+\pi^-p(p)$ events the simultaneous detection of one or more nucleons will allow us to place even more stringent conditions, once again effectively enhancing the ρ^0 channel.

1. The two main ρ^0 production channels, $^3He(\gamma_t, V)^3He$ and $^3He(\gamma_t, V)p(pn)_{sp}$ generate *predominantly* two-track events, and so the detection of one or more nucleons associated with FSI, Δ or N^* decay inherently discriminates against these physics background processes. This is particularly true for the exclusive reaction. In addition, there are regions of phase space where the recoiling ^3He may be detected.

2. The coplanarity criteria for the $\pi^+\pi^-p(p)$ events which we will employ, in regions of phase space where the recoiling nucleon(s) from the $^3He(\gamma_t, Vp)(pn)_{sp}$ reaction fall within the CLAS acceptance, are:

$$(\vec{p_\gamma} \times \vec{p_p}) \cdot (\vec{p_{\pi^+}} + \vec{p_{\pi^-}}) \tag{5}$$

$$(\vec{p_\gamma} \times \vec{p_p}) \cdot (\vec{p_{\pi^+}} - \vec{p_{\pi^-}}) \tag{6}$$

$$(\vec{p_\gamma} \times \vec{p_{\pi^+}}) \cdot (\vec{p_p} \times \vec{p_{\pi^-}}). \tag{7}$$

For events coming from vector meson production on a single nucleon, we expect the angle defined by equation (5) to be a narrow peak centered at 90° with a width determined from the Fermi momentum of single protons in ^3He and the experimental resolution. For competing multi-nucleon background processes, this correlation should be much weaker. This is shown in Figure 9, where the

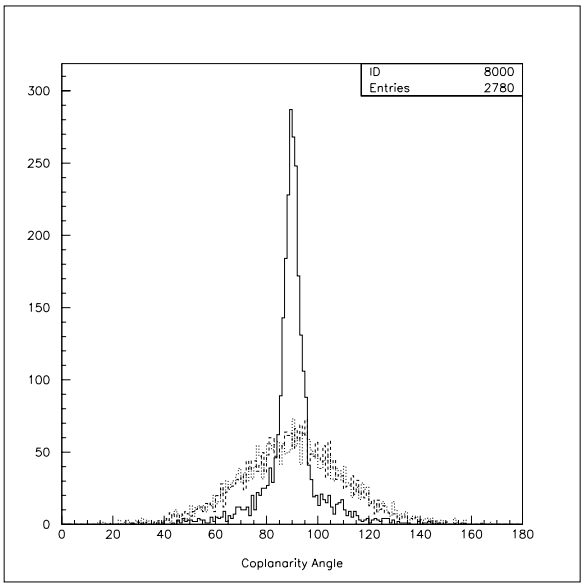

Figure 8: Coplanarity angle, from equation (5), for $\pi^+\pi^-p$ events. The solid line is for the ρ^0 production reaction, the dotted line is for the $\Delta\Delta$ reaction and the dashed line is for the FSI affected process. These are MC simulations using the CLAS simulation package, as explained in Section 5.3.

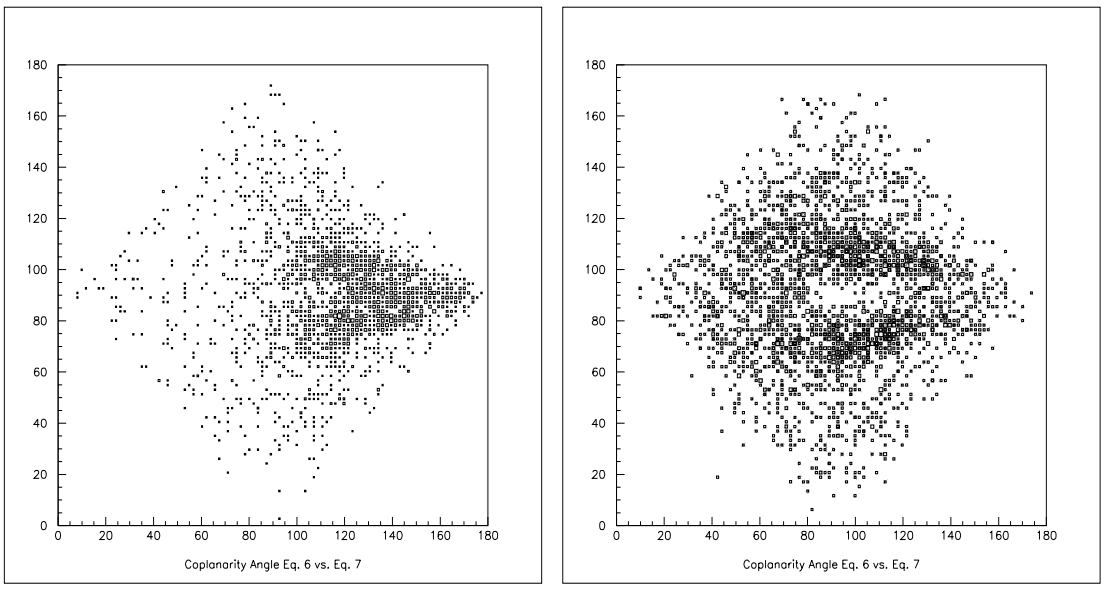

Figure 9: MC simulations, as in the above figure, of the coplanarity angles for $\pi^+\pi^-p$ events. Panels (a) and (b): the coplanarity angle calculated from equation (6) versus that of equation (7) for the ρ^0 production reaction, and quasifree N^* plus single Δ reactions, respectively.

solid curve is for the ρ^0 reaction discussed here, and the other curves are for $\Delta\Delta$ and ρ^0-driven FSI background reactions.

On the other hand, the combined information from equations (6) and (7) can be used as a filter in the analysis to separate the ρ^0 from the quasifree N^* and single-Δ processes. This is illustrated in Figure 9, where these two coplanarity angles are plotted against one another in panels (a) and (b) for the ρ^0 meson, and quasifree N^* plus single Δ channels, respectively.

3. Invariant Mass Tests. Again, for $\pi^+\pi^-p$ events we may accentuate the foreground reaction by placing suitable cuts on the correlation of the invariant mass of the $p\pi^+$ and $p\pi^-$ pairs. One such example is shown in Figure 10. The left plot is for the ρ^0 reaction discussed here, and the right hand plot is for the $\Delta\Delta$ reaction.

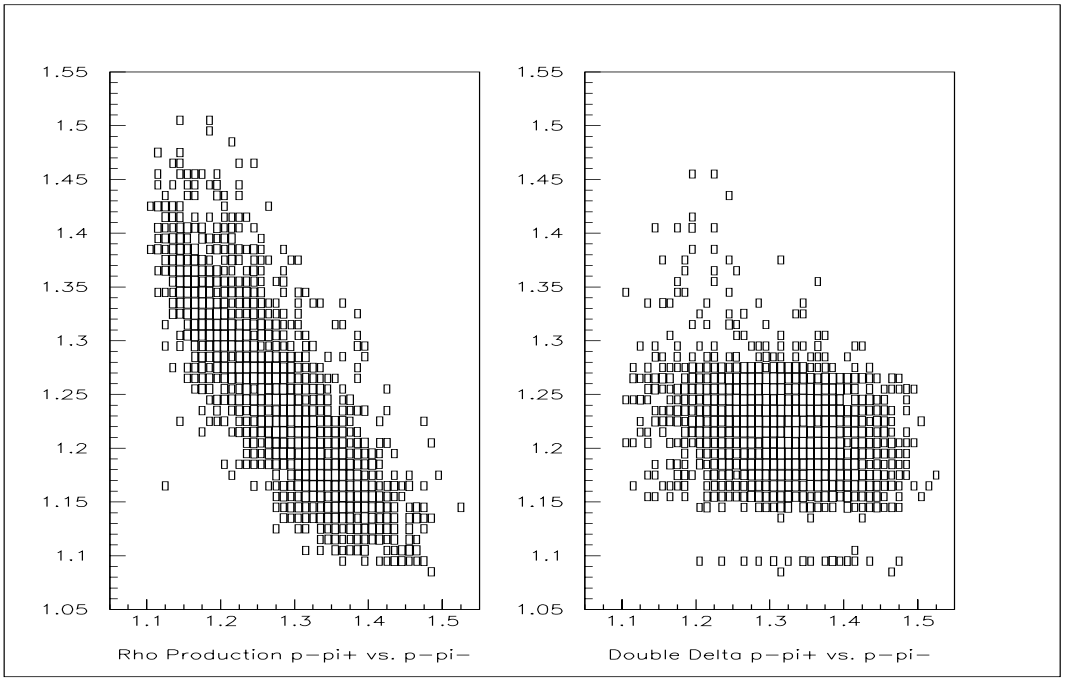

Figure 10: Invariant mass of the $p\pi^+$ pair versus that of the $p\pi^-$ pair for: left, the foreground (ρ^0) and right, the background ($\Delta\Delta$) processes. These are simulated events, as in Figure 9.

4.2.4 Final State Interactions

One of the prime motivating factors in the pursuit of the leptonic $V \to e^+e^-$ decay channel is the lack of pronounced FSI compared to the hadronic channel. In this

section, we present physics arguments which support the TAGX MC fitting results that show no preference for FSI processes in the hadronic channel reactions.

1. One of the dominant FSI processes in nuclei is pion absorption, $\pi^+NN \to NN$. This results in the removal of the event from our trigger and does not represent a problem, as our method of $m^*_{\rho^o}$ extraction is independent of σ_ρ.

2. In the $^3He(\gamma_t, V)^3He$ reaction, the forward peaked $\pi N \to \pi' N'$ scattering is suppressed by simple DWIA arguments, as it involves essentially zero momentum transfer. Inelastic πN scattering (pion production) is discriminated against by missing mass cuts.

3. In the $^3He(\gamma_t, Vp)(pn)_{sp}$ reaction, if the four-momentum is large enough to change the extracted m_{ρ^o}, the FSI and $\rho^0 \to \pi^+\pi^-$ channels can be separated based on their different kinematical signatures which result in the population of different regions of phase space. Indeed, this has been verified in the TAGX analysis of the $^3He(\gamma_t, V)p(pn)_{sp}$ reaction, which is less restrictive, and, in principle, more difficult to analyse than the $^3He(\gamma_t, Vp)(pn)_{sp}$ channel.

4. Finally, if $\pi N \to \pi' N'$ events survive all cuts and if the momentum transfer to the struck nucleon is large enough to affect $m_{\pi^+\pi^-}$, the p-wave signature of the dipion system will also be lost. A clean p-wave signature is final proof of minimal FSI.

5 The Experiment

5.1 Experimental Parameters

In Table 4, we list the basic requirements for the experiment. This information was employed in the Monte Carlo simulations and count rate estimates, discussed later in this section. A matter of importance is that the tagger should be operated using the entire tagging range from 20% to 95% of the endpoint energy. This will allow us to probe deep into the subthreshold region and will permit access to regions where background reactions dominate, providing information that will be used in the deconvolution of the data. It will also lead to coherent production of the ρ^0 and ω, which will be used as a check of the experimental consistency and resolution. The coherent ω signature will also assure us that the ϕ can also be identified subthreshold, since coherent ϕ production is not accessible in the range of photon energies specified here.

5.2 Trigger

As already mentioned above, the optimum condition for this experiment requires two charged particles in the trigger, and an open neutral trigger. This will ensure

Table 4: Proposed Experimental Parameters.

Electron Energy	1.6 GeV
Photon Energy Range	0.32 - 1.52 GeV (0.20-0.95E_o)
Beam current	8 nA
Number of tagged photons	$10^7\gamma/s$
E93-044 Target density	1.0 g/cm^2
E93-044 Target material	liquid ^3He

that events of the types $\pi^+\pi^-$, $\pi^+\pi^-\pi^0$ and $\pi^+\pi^-p$ will be accepted, as well as those where additional nucleons/pions emerge. The sorting of the different reaction channels will be performed off-line. A detailed trigger simulation along the lines of that performed for E93-031 [48] has been performed and continuous refinements are being incorporated.

The optimal trigger as such is rather restrictive. However, as verified in the "leptonic-background free" conditions encountered in the *g6* running period (which ran with a two-particle trigger), if the accidental rates and the DAQ deadtimes are low while the photon flux is maintained high, then a single charged particle trigger may be also considered. The recent CLAS achievement of 1.5 KHz DAQ rate at 20% deadtime, is indeed very encouraging. If, in addition, the accidental rates due to leptonic background can be kept low, then a single charged particle trigger can be employed.

5.3 Acceptance Studies

The events were generated with codes based on the GENBOD package. For each reaction considered, 50000 events were generated, taking into account the ^3He Fermi distribution for single nucleons in ^{3}He. These events, in turn, were fed into the CLAS detector simulation package, GSIM. The resulting pristine output file was then analyzed with the Hall B analysis package, RECSIS, the final result being an ntuple file for each generator. We note that no trigger requirements were imposed in the RECSIS analysis; this was handled entirely within the subsequent ntuple analysis.

5.3.1 Optimal Magnetic Field and Tagger Energy

The objective of these studies is to optimize the acceptance for the foreground reactions by looking at its dependence on the magnetic field of the torus and the tagged photon energy region. In general, with positive particles bending outward, the geometrical acceptance for protons is not drastically affected by choice of field

strength. However, this is **not** necessarily the case for pions, where the π^+ are bent outward and the π^- inward and *away* from the detectors.

We define the acceptance in the usual way:

$$\epsilon = \frac{N_{\rm acc}}{N_{\rm gen}} \tag{8}$$

where $N_{\rm gen}$ is the total number of events generated and $N_{\rm acc}$ represents the numbers of events accepted after passing all cuts.

We simulated ϵ at $E_\gamma = 0.8$, 1.0 and 1.2 GeV, and at B-field values of +0.25, +0.50 and +0.90 times the nominal field strength for the ${}^3He(\gamma_t, \rho^0)p(pn)_{sp}$ reaction, and for a shifted ρ^0 mass of 600 MeV/c^2. The results are shown in Table 5 and plotted in Figure 11. The columns are labelled according to the particles detected in CLAS. The final column, is the total geometrical acceptance for the combined $\pi^+\pi^-$, $\pi^+\pi^- p$ and $\pi^+\pi^- p(p)$ events.

Table 5: Magnetic field acceptance studies for $m^*_{\rho^0} = 600$ MeV/c^2.

${}^3He(\gamma_t, \rho^0)p(pn)_{sp}$				
B/B$_\circ$	$\epsilon_{\pi^+\pi-}$	$\epsilon_{\pi^+\pi^- p}$	$\epsilon_{\pi^+\pi^- p(p)}$	Total ϵ $(\Sigma\rho^0)$
	$E_\gamma = 0.8$ GeV			
+0.25	12.8%	8.8%	0.7%	22.3%
+0.50	9.4%	6.4%	0.4%	16.2%
+0.90	4.2%	2.2%	0.2%	6.6%
	$E_\gamma = 1.0$ GeV			
+0.25	8.5%	11.0%	3.0%	22.5%
+0.50	6.5%	7.9%	2.0%	16.4%
+0.90	3.1%	3.1%	0.7%	6.9%
	$E_\gamma = 1.2$ GeV			
+0.25	5.8%	11.3%	6.0%	23.1%
+0.50	4.2%	7.8%	3.4%	15.4%
+0.90	2.1%	3.1%	1.3%	6.5%

From this table, we note several important features. The first is that the acceptance of the $\pi^+\pi^-$ channel drops by a factor of two from 0.8 GeV to 1.2 GeV, whereas that for the $\pi^+\pi^- p$ channel increases by 30% over this region and the $\pi^+\pi^- p(p)$ also increases, but by a factor of eight. These features are understood by noting that events that are lost from the $\pi^+\pi^-$ sample end up in the $\pi^+\pi^- p$ events because the participating proton gains enough energy to make it into the CLAS acceptance. A similar exchange occurs between the $\pi^+\pi^- p$ and $\pi^+\pi^- p(p)$ subsets. The combined gain and loss of events in the $\pi^+\pi^- p$ channel, due to its two neighbor channels, results in an overall 30% gain.

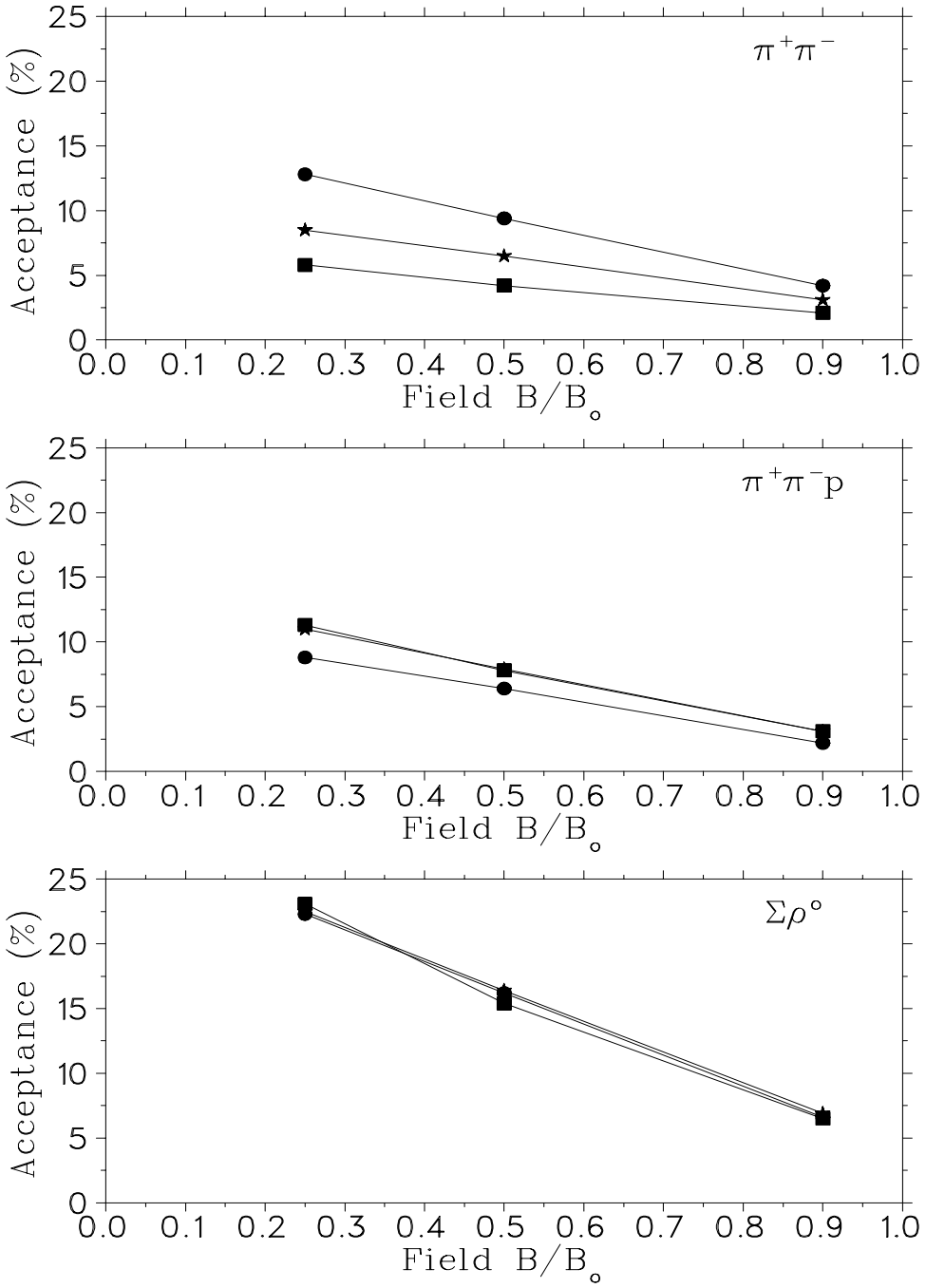

Figure 11: Simulated CLAS acceptance for the $^3He(\gamma_t, \rho^0)p(pn)_{sp}$ reaction as a function of magnetic field. The circles, stars and squares represent the E_γ at 0.8, 1.0 and 1.2 GeV. The top and middle panels are for the $\pi^+\pi^-$ and $\pi^+\pi^-p$ channels, respectively, whereas the bottom panel represents the total efficiency from Table 5.

The second – and most important – point is that the acceptance for both $\pi^+\pi^-$ and $\pi^+\pi^- p$ drops dramatically as a function of $B/B_\circ$: we lose a factor of three in acceptance from +0.25 to +0.90. Moreover, this loss is not uniform: it affects different regions of phase space in a different manner, which is detrimental to this experiment, especially for the ω and ϕ analyses. As explained above, detecting one or both of the final state protons is an essential advantage in suppressing the background processes. Finally, we have examined the affect of the field on the energy resolution and we have determined that it is rather insignificant.

We conclude that the optimal field for the ρ^0 channel is at $B/B_\circ = +0.25$. The same will hold for the ω due to the extra π^0 in the decay, which participates in the sharing of the available kinetic energy. Any significant reduction in the ω mass, either due to in-flight or bound state mechanisms, will further reduce the mean pion momenta, thus making the low field setting even more critical for acceptance maximization. The low field constraint dictates the amount of dedicated beamtime requested.

5.3.2 Geometrical Acceptance Studies

In Table 6, we list the acceptances of the foreground and background reactions, as described in Section 4.2, for the $\pi^+\pi^-$ events, the $\pi^+\pi^- p$ events, and the sum of the two. As is apparent in this table, the acceptance for the foreground channels is quite satisfactory. As a further check of our MC analysis procedure, the $\omega \to \pi^+\pi^-\pi^0$ and the breakup ρ^0 production leading to the $\pi^+\pi^- p$ channel were also simulated with the FASTMC code [49], and the results were in agreement with those shown in Table 6.

Table 6: Geometrical Acceptance of CLAS for Channels Described in Section 4.2, for $B/B_\circ$=+0.25, E_γ = 1.0 GeV and $m^*_{\rho^o}$ = 600 MeV/c^2.

Label	$\epsilon_{\pi^+\pi^-}$	$\epsilon_{\pi^+\pi^- p}$	Sum
Exclusive ρ^0 production	18%	0%	18%
Breakup ρ^0 production	9%	11%	20%
Exclusive ω Production	5%	0%	5%
Breakup ω production	4%	3%	7%
Single Δ production	9%	9%	18%
Quasifree N^* production $^{(*)}$	5-8%	3-8%	8-16%
Double Δ production	6%	11%	17%
Incoherent $\pi^+\pi^-\pi^0$ (Exclusive)	14%	0%	14%
Incoherent $\pi^+\pi^-\pi^0$ (Breakup)	3%	2%	5%
$^{(*)}$ indicates different resonances considered			

5.4 Beam Time Estimate

In our beam time estimate, we have used the acceptance of the $\pi^+\pi^-p$ channel at E_γ=800 MeV (ϵ=0.12, Figure 11), which was calculated for $m^*_{\rho^o}$=600 MeV/c^2. Furthermore, we have estimated that the efficiency of survival of the different offline cuts (coplanarity, missing momentum, angular correlations, missing mass, etc.) is η=0.5.

The MC fitting procedure assumes constant matrix elements within each tagged photon energy bin. In this experiment, we plan to use 20 MeV bins. This finer photon energy bin, compared to the 80 MeV used in the TAGX analysis, will allow a more reliable fitting of the simulations of different processes, both because the matrix elements vary very little in such small increments, and because the larger number of data allow a higher fitting confidence in the overall MC fitting algorithms. Furthermore, an accurate determination of $m^*_{\rho^o}$ from the $l = 1$ angular distribution analysis (see Figure 3) can be obtained by binning the invariant mass in 50 MeV/c^2 (or even finer) intervals, compared to 100 MeV/c^2 of the TAGX analysis, *for each of the 20 MeV energy bins around the critical subthreshold regions for nucleonic and nuclear sources of modification*. This will allow a more definitive interpretation of the collected data. With this binning in mind, a 5% (high confidence) measurement in each bin may be achieved by requiring N_{ρ^0}=10000 ρ^0 events (after most of the cuts have been imposed).

The precision of the proposed experiment will far exceed the TAGX results, as shown in Figure 12. In this figure, the results from the two TAGX experiments on ^3He are shown [31, 32], and are compared to a simple model calculation which assumes production on a nucleon in ^3He by folding the nucleon density distribution, the single nucleon Fermi momentum distribution in ^3He, and the phase space available due to the beam energy and TAGX acceptance [24]. As a comparison, the expected CLAS results are also shown, as if they follow the simple model curve. Such quality data sets can be effectively used to investigate specific physics processes leading to medium modifications, and this capability comprises another unique feature of this experiment.

The photon flux from Table 4 is spread over a 1200 MeV wide bite, and we have scaled it to the 20 MeV wide bin assuming a flat distribution of photons in this tagging energy region. We have also assumed an average cross section σ= 4 μb for a modified mass $m^*_{\rho^o}$=600 MeV/c^2 at 800 MeV, which is consistent with the analyses of references [31, 32] and is shown in Figure 12. The cross sections for ω and ϕ have been normalized to that of the ρ^0 assuming the cross section ratios derived from photoproduction on the proton for ρ^0, ω and ϕ scale similarly in the subthreshold region. This results in σ_ω= 0.44 μb and σ_ϕ= 0.11 μb, respectively.

The beam time required under the assumptions and criteria above, is calculated using the following relation:

$$\sigma = N_{\rho^0}/[R_\gamma \cdot t \cdot \epsilon \cdot \eta \cdot N_{nuc} \cdot \alpha] \tag{9}$$

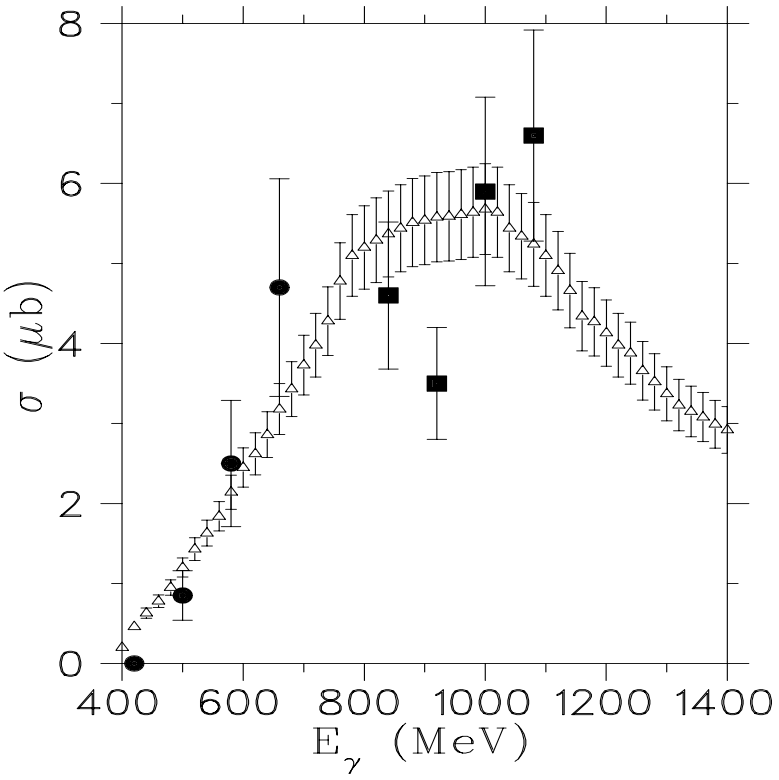

Figure 12: The cross section for the $^3He(\gamma_t, \rho^0)p(pn)_{sp}$ channel, assuming a mass of 600 MeV/c^2 for the shifted ρ^0 meson. Filled boxes and circles represent the numbers extracted with the MC fitting technique from references [31] and [32], respectively. The open triangles depict the expected CLAS results from the $^3He(\gamma_t, Vp)(pn)_{sp}$ channel, assuming that they follow the simple model calculation, which has been arbitrarily normalized to the data distribution. A 10% overall systematic error for the CLAS results has been assumed in this simulation.

where $N_{nuc} = 2 \times 10^{23}$ nuc/cm^2 and $R_\gamma = 1.7 \times 10^5 \gamma/s$, are the number of target nuclei and photon flux, respectively, in a 20 MeV wide photon energy bin. The branching ratio for the particular decay is represented by the variable α.

From the above equation, we determine the beam time t required is 420 hours. It should be emphasized that, at the same time, the number of ω (ϕ) mesons detected via the $\pi^+\pi^-\pi^0$ channel will be approximately 500 (30), under the same E_γ binning. Thus, the beamtime on target calculated for the ρ^0 (our primary objective), is the minimum beam time required for a serious effort on the ω and a conclusive feasibility study for the ϕ. The ω and ϕ events will clearly need to be binned in larger E_γ and invariant mass bins in order to improve statistics, but unless the width is increased in the medium, only a few modified ϕ mesons are expected to be observed.

This amount of beam time will also assure a well populated sample of $\pi^+\pi^-$

events coming from the exclusive ρ^0 production on ^3He. In the case of a bound ω decay into $\pi^+\pi^-\pi^0$, the result will most likely be the breakup of ^3He, therefore the total acceptance of 7% will represent the most likely scenario. As a result, the quoted number of events of 500 per 20 MeV E_γ bin is actually a lower estimate.

We request 420 hours for ^{3}He running in Hall B with the CLAS magnetic field at 0.25B$_\circ$, and E_γ=320-1520 MeV. This estimate does not include data acquisition dead time nor CEBA and Hall B beam delivery inefficiencies. As this proposal is being written, we believe that 150 hours can be collected in parallel with the already approved g3 *beamtime. This would reduce the hours of* **beamtime requested for this experiment to 270 hours.**

6 Conclusions

Subthreshold photoproduction of vector mesons off nuclei is the most precise and promising method of investigating mass modifications in the presence of hadronic matter. Unlike the heavy ion results from CERN, where only invariant mass distributions of dilepton production were considered in the analysis, the experiment in this proposal will analyze several additional sensitive variables simultaneously, which effectively constrain the alternative interpretations of the results. The hadronic decay channel has the advantages of large branching ratios, good final signal to noise ratio, and it carries information inherent to the ρ^0 meson, via its spin in the angular distributions. This spin property can provide an assumption independent $m^*_{\rho^o}$ extraction via the $l = 1$ signatures, and can also probe possible spin dependent effects on mass modification. The nucleonic origin of large mass modifications reported by the TAGX collaboration and the subject of possible bound states for vector mesons in nuclei can only be probed by such subthreshold production experiments. Finally, the selection of ^3He as our target, together with the multi-observable analysis, minimizes FSI interactions which could interfere with the sought-for modified V-meson signatures.

The experience from the TAGX analysis, coupled with the intrinsic advantages of CLAS and the extensive MC simulations in this proposal, clearly show that the ρ^0 signal can be successfully extracted from the background generated by other processes. The large phase space acceptance of CLAS and the coplanarity possibilities open in the $\pi^+\pi^-p$ data sets, allow analysis methods unique to this field. The extraction of mass modifications for the ω and ϕ is more difficult, but given sufficient statistics in appropriate regions of phase space, the chances of success are good, more so for the former than the latter.

Even though the TAGX results point to an unexpectedly large mass reduction for the ρ^0, several important questions are still unanswered and some new ones have been brought forward and which can only be answered by the proposed experiment:

- **Precision of expected CLAS data:** The quality and quantity of the CLAS data will be so much better than that from the TAGX experiment, that we

expect to be able to provide a definitive and precise $m^*_{\rho^o}$ measurement, and the results will serve as valuable input to theoretical models in terms of the vector meson mass dependence as a function of hadron density. They will also help decide which, of all the theoretical works, is worth pursuing further.

- **Separation of mass and width modifications:** The TAGX experiment could not make firm conclusions on the relative roles that the mass and/or width modifications play. The proposed measurements will provide conclusive results for the ρ^0 because of the more surgical nature of the analysis, especially in connection to the pion emission angle (the $l = 1$ signature) in the dipion center of mass, afforded by an invariant mass binning of 50 MeV/c^2 or better. The CLAS out of plane acceptance and the analysis of three-track events will be instrumental in this effort.

- **Nucleonic versus nuclear sources of modifications:** The separation of the effects on mass and width for the ρ^0 in the exclusive and breakup reactions, respectively, with increased statistics and confidence, will provide answers to the questions raised by the TAGX results. Namely, do we indeed observe mass modification due to the nucleonic effect, which masks the weaker nuclear effect?

- **Bound ω states in ^3He:** The issue of bound vector meson states in nuclei is a very recent one and it greatly affects our understanding of nuclear physics. A bound vector meson state is a direct signature of deep scalar fields which are intrinsic to *QHD*, and the subthreshold production of the ω will be the testbed of such assertions. It is beyond doubt that if the ω is produced at rest with respect to the nucleus and it becomes bound, the signature of such a bound state will show up very clearly. The background to the $\omega \rightarrow \pi^+\pi^-\pi^0$ reaction, either by itself or associated with detection of emitted nucleon(s), is so small that even an in-medium decay fraction of a few percent will be observed with confidence. A bound state, by its very own nature, will result in large in-medium decay fractions, compared to in-flight medium modifications. As a result, these two different physics phenomena will have different experimental signatures.

- **The modifications for the ϕ meson:** Due to long decay length and small expected mass modification due to low strangeness content of the nucleon, as well as low production cross section, the search for ϕ modifications is more exploratory in nature. If, however, theoretical calculations which predict large modification of the width of the ϕ to 30 MeV/c^2 [34] or 45 MeV/c^2 [18] are accurate, the in-medium decay fraction of the produced ϕ mesons will increase substantially. Such an observation is very valuable on its own merit and it becomes even more exciting in combination with the other two vector mesons, due to the strangeness content of the ϕ. Nevertheless, ϕ modifications will be very difficult to extract.

Appendix A - Modifications Probed with Hadrons

The experiments below have inferred the presence of medium modifications but were not entirely conclusive, as other conventional mechanisms could also explain the data, at least in part. Nevertheless, they are noteworthy because they hint at medium modifications in a variety of nuclear systems.

The Earliest Results: The DLS collaboration at the BEVALAC [50] was the first to look for vector meson mass modifications in heavy ion experiments. The dilepton production cross sections were analyzed in terms of conventional transport mechanisms which did not include any ρ^0 mass modifications, but provided agreement with the data [51, 52]. Recently, however, a reanalysis has resulted in an increased dilepton production cross section [53]; whether the new results can still be accommodated within similar conventional transport mechanisms or whether ρ^0 mass modification is required, is not yet known.

Heavy Ions at CERN: The most interesting heavy ion results come from the CERES [25, 26] and HELIOS-3 [27] collaborations at CERN. The $p+Be$ and $p+Au$ results at 450 GeV/u did not exhibit any unusual invariant mass features. On the other hand, the corresponding $S+Au$, $S+W$, and $Pb+Au$ data are quite different: their most striking feature is an enhancement in the invariant mass of the dilepton (e^+e^- or $\mu^+\mu^-$) system. Conventional calculations underpredict the data in the 250-500 MeV/c^2 region, unless ρ^0 mass modifications are included [54]. However, there are many caveats connected to this result that are associated with refinements to the conventional picture [55]. Nevertheless, these heavy ion results are inconsistent with a mere superposition of *p*-*p* interactions, a fact that possibly indicates a collective phenomenon: partial restoration of chiral symmetry. Improvements in the energy resolution of CERES have been approved and a follow-up experiment is eagerly awaited.

K^+-nucleus scattering: The Brown-Rho scaling in equation (1) was first applied to explain an enhancement in the K^+-^{12}C elastic cross section [28]. Apparently, it was conjectured that both the elastic and total cross sections of this reaction are sensitive to the nuclear density dependent effective masses of the light vector mesons.

Results from IUCF: Polarization transfer measurements in $\vec{p}-^{28}Si$ scattering have been carried out at IUCF [29] in order to investigate whether the effective $N-N$ interaction is altered in the nuclear medium. DWIA calculations showed that only the in-plane spin-transverse differential cross section was predicted well, whereas the spin-transverse and spin-longitudinal cross sections were underpredicted by 20% and overpredicted by a factor of two, respectively. The investigation of strong relativistic mean fields and Pauli blocking were insufficient to rectify the situation on their own accord. Only the inclusion of a reduction of the ρ^0 mass in the t-matrix resulted in a substantial improvement in the description of the data, although the changes suggested by the data did not correspond to the same reduced mass for each amplitude. Further work needs to be done on such indirect measurements by applying more sophisticated calculations.

Appendix B - Comparison to E94-002 at Hall B

The approved Hall B experiment E94-002, "Photoproduction of Vector Mesons off Nuclei", is similar, in topic, to the one proposed here. There are, however, also major differences in both the physics objectives and the methodology.

The energy range of the photons in E94-002 is 1.2-2.2 GeV. The three vector mesons will be detected by their leptonic decay channels $V \rightarrow e^+e^-$ at energies above threshold for the ρ^0 and ω. The ϕ meson, on the other hand, is open to subthreshold production, although this mechanism was not an original intention.

It is the very nature of the subthreshold energy regime that really sets our proposal apart from E94-002. The mass modification induced by the nucleonic density can only be probed at subthreshold energies. As such, we will investigate this new medium effect, which cannot be probed at higher energies and higher Lorentz boost regimes for the vector mesons. In a similar argument, investigation of postulated vector meson bound states for the ρ^0 and ω mesons are not effectively probed at high E_γ regions. However, the nuclear mass modification effect is accessed in a similar way between this proposal and E94-002, but with a totally different methodology. With the TAGX results pointing to a large mass modification, the present proposal is less exploratory and more precision oriented in nature than the earlier E94-002.

The choices of energy range and massive targets in E94-002 bring that experiment in the coherent production regime, which dominates vector meson production. These coherent events can be suppressed to an extent by imposing cuts on -t. The detection of the leptonic decay products, has, on one hand, the benefit of allowing the use of heavy nuclei as targets, in order to maximize the probability of vector meson decay within the nuclear target. The experiment is also more sensitive to ρ^0-ω mixing, than our proposed experiment. On the other hand, however, the leptonic channel imposes a severe penalty on the final statistics due to the very low branching ratios and due to the production of e^+e^- pairs via the Bethe-Heitler process, which is also more pronounced for heavier nuclei. The latter process can be suppressed by demanding the detection of the recoil nucleon in the production process, a technique which also suppresses coherent production to a degree. The penalty of this technique is that a further loss of acceptance by almost 50% is imposed.

Both experiments are capable of pursuing ϕ production at subthreshold energies. Even though the ϕ modification is the most difficult to extract, an agreement between the two experiments will provide valuable and verifiable information on strangeness effects in nuclear physics. This will be particularly true if the large increase in the width of the ϕ meson in nuclei, as have been proposed by [18, 34], turn out to be correct.

E94-002, then, will attempt to measure the *nuclear effect* of the vector meson mass modification and as such, it is seeking to determine the same effect as the exclusive $^3He(\gamma_t, V)^3He$ reactions in our proposal. In this last respect only, the two approaches are complementary. Each one has its own unique technical problems and each one uses a different approach in probing nuclear medium effects.

Appendix C - Experiments at Other Facilities

Experiments pursuing the study of modifications of vector mesons in nuclear matter have been proposed or are being carried out at a number of diverse accelerator facilities. These are explained here briefly. The list below is impressive in that it demonstrates the interest on this topic in several subfields of subatomic physics.

1. *KEK:* Very similar in nature to the Hall B experiment: lepton pairs in heavy nuclei will be examined in KEK-PS experiment E325 [56]. One interesting feature is that this group proposes to measure the $\Gamma(\phi \to e^+e^-)/\Gamma(\phi \to K^+K^-)$ ratio. Since m_ϕ is very close to $2m_K$ in the vacuum, any modification of the ϕ or K masses will affect this ratio substantially as a function of mass number. Experiments at GSI also plan to investigate this ratio.

2. *GSI, Darmstadt:* The HADES [57] di-electron spectrometer will be used to investigate lepton pair emission in relativistic heavy ion collisions and dilepton production in elementary reactions. In several cases, these experiments need to detect photons as well from the η-Dalitz decays, by using the TAPS photon detector.

3. *CERN:* The CERES/NA45 and NA50 experiments [26] continue to study both the e^+e^- and $\mu^+\mu^-$ channels, over the invariant mass region from threshold to the mass of the J/ψ.

4. *BNL:* Preliminary data from AGS-BNL has been reported [58] on the K^+K^- decay channel of the ϕ meson, indicating a possible (less than 1%) downward shift in the ϕ mass in central $Si + Au$ collisions.

References

[1] DeTar CE, *Quark Gluon Plasma 2*, ed. R. Hwa. Singapore: World Scientific (1995).
K.J. Escola, Nucl. Phys **A590** (1995) 383c.
F. Wilczek, Physics Today, April 1998, p.11.

[2] F. Douglas Swetsy *et al.*, Astro. Phys. Jour. **425** (1994) 195.

[3] M. Prakash *et al.*, Phys. Rep. **280** (1997) 1.

[4] F. Karsch, Nucl. Phys. **A590** (1995) 367c.

[5] T. Hatsuda and T. Kunihiro, Phys. Rep. **247** (1994) 387.

[6] T. Hatsuda, LAMPF preprint nucl-th/9608037.

[7] C.M. Ko, V. Koch and G. Li, Ann. Rev. Nucl. Sci. **47** (1997) 505.

[8] G.E. Brown, M. Buballa and M. Rho, Nucl. Phys. **A609** (1996) 519.

[9] C. Bernard *et al.*, Phys. Rev. **D45** (1992) 3854.

[10] G.E. Brown and M. Rho, Phys. Rev. Lett. **66** (1991) 2720.

[11] T. Hatsuda and S.H. Lee, Phys. Rev. **C46** (1992) R34.

[12] T. Hatsuda, S.H. Lee and H. Shiomi, Phys. Rev. **C52** (1995) 3364.

[13] T. Hatsuda, LAMPF preprint nucl-th/9702002.

[14] X. Jin and D.B. Leinweber, Phys. Rev. **C52** (1995) 3344.

[15] K. Saito and A.W. Thomas, Phys. Rev. **C52** (1995) 2789.

[16] M. Asakawa and C.M. Ko, Nucl. Phys. **A572** (1994) 732.

[17] M. Asakawa and C.M. Ko, Phys. Rev. **C48** (1993) R526.

[18] F. Klingl *et al.*, Nucl. Phys. **A560** (1997) 527.

[19] J.D. Walecka, Theoretical Nuclear and Subnuclear Physics, Oxford University Press (1995).

[20] B.D. Serot and J.D. Walecka, Adv. Nucl. Phys. **16** (1986) 1.

[21] S.J. Wallace, Ann. Rev. Nucl. Part. Sci. **37** (1987) 267.

[22] P.G. Reinhard, Rep. Prog. Phys. **52** (1989) 439.

[23] K. Tsushima *et al.*, LAMPF preprint nucl-th/9806043 (1998).

[24] Z. Papandreou *et al.*, APS e-print aps1998nov26002, submitted to Phys. Rev. C Rapid Communications.

[25] G. Agakichev *et al.*, CERES Collaboration, Phys. Rev. Lett. **75** (1995) 1272.

[26] J.P. Wurm *et al.*, NA45/CERES Collaboration, Nucl. Phys. **A590** (1995) 103c.

[27] M. Masera *et al.*, HELIOS-3 Collaboration, Nucl. Phys. **A590** (1995) 93c.

[28] G.E. Brown et al., Phys. Rev. Lett. **60** (1998) 2723.

[29] E.J. Stephenson *et al.*, Phys. Rev. Lett. **78** (1997) 1636.

[30] K. Maruyama *et al.*, Nucl. Instr. Meth. in Phys. Res. **A376** (1996) 335.

[31] G.J. Lolos *et al.*, Phys. Rev. Lett. **80** (1998) 241.

[32] G.M. Huber, G.J. Lolos and Z. Papandreou, Phys. Rev. Lett. **80** (1998) 5285.

[33] M. Kagarlis *et al.*, LAMPF preprint nucl-ex/9811010, submitted to Phys. Rev. C.

[34] C. Song, Phys. Rev. **D48** (1993) 1375.

[35] N. Isgur, private communication (1998).

[36] M. Asakawa and C.M. Ko, Phys. Rev. **C50** (1994) 3064.

[37] P.-Y. Bertin, M.V. Kossov, B.M. Preedom *et al.*, "Photoproduction of Vector Mesons off Nuclei", JLab Proposal E94-002.

[38] H. Alvensleben *et al.*, Nucl. Phys. **B18** (1970) 333.

[39] K. Saito,T. Tsushima and A.W. Thomas, Phys. Rev. **C55** (1997) 2637.

[40] B.L. Berman, P. Corvisiero, G. Audit *et al.*, "Photoreactions on ^3He," JLab Proposal E93-044.

[41] K. Saito, T. Tsushima and A.W. Thomas, Phys. Rev. **C56** (1997) 566.

[42] P. Guichon and M. Ericson, private communication.

[43] M.C. Abreu *et al.*, NA38 Collaboration, Nucl. Phys. **A590** (1997) 117c.
M.C. Abreu *et al.*, NA50 Collaboration, Phys. Lett. **B410** (1997) 327 and 337.

[44] D. Luke, P. Soding, Springer Tracts Mod. Phys. **59** (1971) 39.

[45] M. Asai, et al., Zeit. Phys. **A344** (1993) 335.

[46] Y. Wada, representing the SAPHIR collaboration, Particles and Nuclei International Conference, Williamsburg, VA, June, 1996.

[47] D.G. Watts et al., Phys. Rev. C **55** (1997) 1832.

[48] M. Battaglieri *et al.*, *CLAS-Note* 97-006.

[49] E.S. Smith, "FAST Monte Carlo for the CLAS Detector," *CLAS-Note* 90-003.

[50] G. Roche *et al.*, Phys. Rev. Lett. **61** (1988) 1069.
C. Naudet *et al.*, Phys. Rev. Lett. **62** (1988) 2652.

[51] L. Xiong *et al.*, Nucl. Phys. **A512** (1990) 772.

[52] G. Wolf *et al.*, Nucl. Phys. **A517** (1990) 615.

[53] R.J. Porter *et al.*, Phys. Rev. Lett. **79** (1997) 1229.

[54] G.Q. Li, C.M. Ko and G.E. Brown, Phys. Rev. Lett. **75** (1995) 4007.

[55] A. Drees, Nucl. Phys. **A610** (1996) 536c.

[56] KEK-PS E325 Homepage:
http://kupns1.scphys.kyoto-u.ac.jp/∼yokkaich/phi/pub/E325_project.html.

[57] HADES WWW Homepage: http://piggy/physik.uni-giessen.de/hades/.

[58] B. Cole *et al.*, Nucl. Phys. **A590** (1995) 179c.